Published in : Macromolecules (2021), vol.54, n°22, pp. 10415–10427
DOI: 10.1021/acs.macromol.1c01895
Status : Postprint (Author's version)

CO_2-Derived Methylene Oxazolidinone: A Platform Building Block for Functionalizing Ethylene–Vinyl Alcohol Copolymers

Zhuoqun Wang, Bénédicte Vertruyen, Hamid Taghipour, Christophe Detrembleur, and Antoine Debuigne*

Zhuoqun Wang, Hamid Taghipour, Christophe Detrembleur, Antoine Debuigne, Center for Education and Research on Macromolecules (CERM), CESAM Research Unit, Department of Chemistry, University of Liege, 4000 Liège, Belgium;

Benedicte Vertruyen, LCIS, GreenMAT, CESAM Research Unit, Department of Chemistry, University of Liege, 4000 Liège, Belgium

Keywords :

Copolymerization, Copolymers, Hydrocarbons, Monomers, Polymers

Abstract

Ethylene–vinyl alcohol copolymers (EVOHs) are important materials available in a variety of compositions and valued in countless applications. In spite of their great adaptability offered by the adjustment of their ethylene content, the chemical modification of EVOHs is often considered to tune their properties and functionalities in order to meet the stringent requirements of today's applications. While post-polymerization modification of the pendant hydroxyl groups of EVOHs is the prevailing functionalizing strategy, this multistep approach consumes part of the alcohols of EVOHs and remains limited in terms of functions. This work reports a straightforward platform for the synthesis of functional EVOHs, in particular, amino derivatives, involving a CO_2-derived oxazolidinone-containing methylene heterocycle, namely, 4,4-dimethyl-5-methyleneoxazolidin-2-one (DMOx). The ethylene/DMOx and ethylene/vinyl acetate/DMOx copolymerizations were implemented by conventional and reversible deactivation radical copolymerization. The resulting oxazolidinone-containing ethylene-based copolymers were then converted into novel vicinal amino alcohol-functional EVOHs via hydrolysis of esters and oxazolidinones. A selective post-modification method of these 1,2-amino alcohol-functional EVOHs into their oxazolidine counterparts is also reported. Finally, the peculiar thermal and solution properties, including pH-responsiveness, of these novel vicinal amino alcohol- and oxazolidine-functional EVOHs as well as oxazolidinone EVAs are discussed.

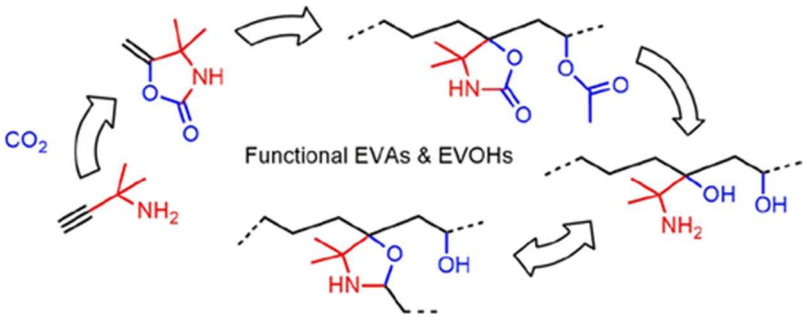

Published in : Macromolecules (2021), vol.54, n°22, pp. 10415–10427
DOI: 10.1021/acs.macromol.1c01895
Status : Postprint (Author's version)

Introduction

Ethylene−vinyl alcohol copolymers (EVOHs) are commonly produced by radical copolymerization of ethylene (E) with vinyl acetate (VAc), followed by saponification of the pendant ester groups. The global EVOH market was valued at about one billion USD in 2020, and a variety of semicrystalline EVOHs with different ethylene contents are used in many applications especially in the packaging of food, cosmetics, and drugs, due to their excellent barrier properties to oxygen, nitrogen, and carbon dioxide.[1−5] These EVOHs also combine interesting features such as transparency, processability, antistatic properties, film-forming capacity, and high resistance to hydrocarbons, oils, and organic solvents.[2,5] Moreover, their biocompatibility and nontoxicity make EVOHs valuable materials in the biomedical area[6−9] notably in drug release,[10,11] protein separation,[12−14] and water purification.[15]

While EVOHs are suitable for many uses, their chemical modification may be necessary to fine-tune their properties and functionalities in order to meet the more and more stringent requirements of today's cutting-edge applications. The prevailing functionalization strategy of EVOHs consists in the chemical modification of its abundant pendant hydroxyl groups.[16] The latter was notably reacted with acyl chloride,[17] carboxylic acid,[18,19] anhydride,[16,20,21] aldehyde,[8] cyanuric chloride,[8,22,23] lactone,[24] and carbonate,[25] to name a few. For example, glycopolymers were prepared from EVOHs via a sequential reaction with phthalic anhydride and amino-saccharides.[26,27] Some amine-functionalized EVOH nano-fibrous membranes of interest for the capture of lipophilic toxins were produced via activation with cyanuric chloride and functionalization by 1,3-propanediamine, hexamethylenedi-amine, and diethylenetriamine.[23] Thermoresponsive EVOH-based microporous membranes were also elaborated via immobilization of the ATRP initiator through acylation of EVOH followed by grafting from radical polymerization of *N*-isopropylacrylamide.[28] Although efficient, these approaches consume some hydroxyl moieties of EVOHs, functions which endow important properties such as hydrophilicity. Copolymerization is another common strategy to introduce functionalities into polymers. Compared to the post-modification method, the copolymerization approach is more efficient in terms of the number of reaction steps and offers a better control of the copolymer composition and of the distribution of the functions along the chains. Nevertheless, this approach has been neglected for the production of functional EVOHs. Indeed, only few reports describe the radical terpolymerization of E and VAc with a third monomer such as methyl acrylate[29,30] or acrylonitrile.[31] Moreover, these reactions took place at high pressure and the resulting terpolymers were not converted into their EVOH counterparts. Exo-methylene cyclic compounds are an interesting class of comonomers whose radical (co)polymerization has been investigated by various research groups.[32−44] Moreover, hydrolysis of some pendant heterocyclic groups generates two functions per repeating units.[32,45−49] For example, vinyl carbonates,[46] vinyl lactones,[47] and vinyl oxazolidinones[48] were successfully copolymerized with vinyl acetate (VAc) leading to diol-, acid-, or amino-functionalized poly(vinyl alcohol)s (PVAs), respectively. Recently, vinyl carbonates were also copolymerized with ethylene leading to polyethylene (PE) decorated by vicinal pendant diol groups after hydrolysis.[45] These exo-methylene cyclic monomers, however, have never been considered for the preparation of functional EVOHs.

Herein, we report a straightforward strategy for the synthesis of functional EVOHs, in particular amino-functional derivatives, based on 4,4-dimethyl-5-methyleneoxazolidin-2-one (DMOx), a methylene heterocycle produced from CO_2 and propargyl amine. First, we explored the incorporation of DMOx

Published in : Macromolecules (2021), vol.54, n°22, pp. 10415–10427
DOI: 10.1021/acs.macromol.1c01895
Status : Postprint (Author's version)

into the copolymer chains via its radical copolymerization with E or its terpolymerization with E and VAc. The resulting oxazolidinone-containing copolymers were then hydrolyzed into novel amino-functional EVOH copolymers (**Scheme 1**). The incorporation of the amine functions along the polymer backbone is likely to not only impart valuable properties such as ability to protonate or metal chelation ability but also offer multiple chemical modification possibilities. This was illustrated by the quantitative and selective conversion of the amino-functional EVOHs into oxazolidines. The thermal and solution properties of the parent oxazolidinone-containing ethylene–vinyl acetate copolymers (EVAs), the novel amino alcohol- and the oxazolidine-functional EVOHs were reported. The possibility to prepare functional EVOHs with precise molar masses and compositions by reversible deactivation radical polymerization (RDRP) was also considered, opening new perspectives in the design of well-defined functional ethylene-based copolymers.

Scheme 1. Synthesis of Oxazolidinone EVAs as Well as Vicinal Amino-Alcohol- and Oxazolidine-Functional EVOHs

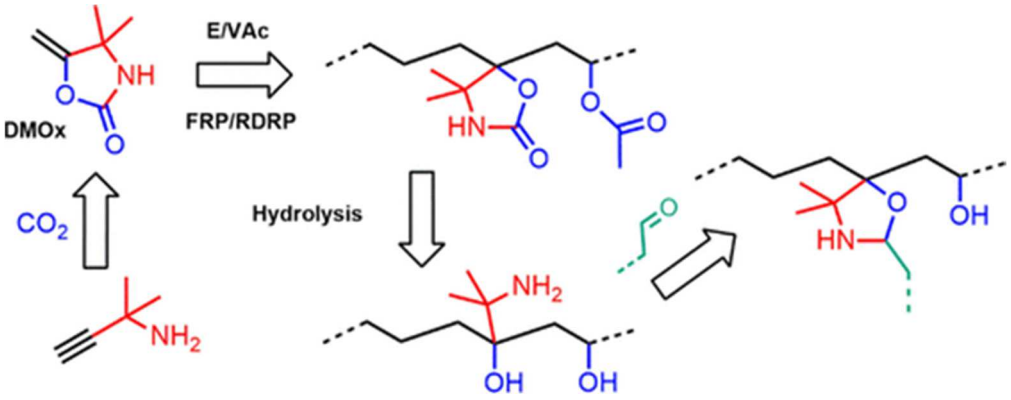

Experimental Section

Materials. Cobalt(II) acetylacetonate ($Co(acac)_2$) (97%, Acros), 1,1-dimethyl-prop-2-ynylamine (90%, Fluorochem), 2,2,6,6-tetramethylpiperidine 1-oxyl (TEMPO) (98%, Aldrich), 2,2′-azobis(4methoxy-2,4-dimethyl valeronitrile) (V-70, $t^{1/2}$ = 10 h at 30 °C) (>98%, Wako), glutaraldehyde solution (25% in water, Aldrich), and hexanal (98%, Aldrich) were used as received. Sodium hydroxide (NaOH, ≥97%, Acros), silica gel for column chromatography (60 Å, ROCC S.A.), tetrahydrofuran (THF, ≥99.9%, VWR), chloroform (>99%, VWR), methanol (MeOH, ≥99.8%, VWR), ethanol (EtOH, ≥99.8%, VWR), *n*-hexane (>99%, VWR), ethyl acetate (≥99.9%, VWR), and acetone (>99%, VWR) were used as received. 2,2′Azobisisobutyronitrile (AIBN) (AIBN, $t^{1/2}$ = 10 h at 65 °C) (98%, Aldrich) was purified via recrystallization in MeOH. Dimethyl carbonate (DMC, >99%, Merck) was degassed and dried over 4 Å molecular sieves prior to use. Dichloromethane (CH_2Cl_2) was degassed and dried over 4 Å molecular sieves. Vinyl acetate (VAc) (>99%, Aldrich) was dried under calcium hydride, purified by distillation under reduced pressure, and degassed by the freeze-drying cycle under vacuum. The alkyl-cobalt(III) adduct initiator ($PVAc_{<4}Co(acac)_2$), [$Co(acac)_2$-$(CH(OAc)-CH_2)_{<4}R_0$], R_0 being the primary radical generated by 2,2′-azo-bis(4-methoxy-2,4-dimethyl valeronitrile) (V-70, Wako), was prepared as described previously[50] and stored as a CH_2Cl_2 solution at −20 °C under argon. Dialyses were carried out

Published in : Macromolecules (2021), vol.54, n°22, pp. 10415–10427
DOI: 10.1021/acs.macromol.1c01895
Status : Postprint (Author's version)

with a Spectra/Por dialysis membrane (pretreated RC tubing 1 kDa). A 23 mL Parr bomb reactor (4749 Acid Digestion Vessel) was used for the base hydrolysis of poly(DMOx-co-VAc) carried out at 120 °C.

Characterization. Size exclusion chromatography (SEC) of polymers was carried out in DMF containing 0.025 M LiBr at 55 °C with a Waters chromatograph equipped with three columns [PSS GRAM 1000 Å (×2), 30 Å], a dual λ absorbance detector (Waters 2487), and a refractive index detector (Waters 2414). The system was operated at a flow rate of 1 mL/min, and polystyrene calibration was used. ^{1}H nuclear magnetic resonance (^{1}H NMR) (400 MHz), power gate proton-decoupled ^{13}C NMR (^{13}C{^{1}H} NMR) (101 MHz), solid-state cross-polarized/magic angle spinning ^{13}C NMR (solid-state ^{13}C CP/MAS NMR) (101 MHz), heteronuclear single quantum coherence (HSQC), and correlation spectroscopy (COSY) spectra were recorded at 298 K with a Bruker AVANCE III HD spectrometer (B_0 = 9.04 T) (400 MHz) and treated with MestreNova software. Fourier transform infrared (FTIR) spectroscopy spectra were recorded on a Thermo Fisher Scientific Nicolet IS5 equipped with an ATR ID5 module using a diamond crystal (650−4000 cm^{-1}). Dynamic light scattering (DLS) was used to obtain the average size of the particles using a Delsa NanoC instrument. Differential scanning calorimetry (DSC) was performed on a DSC 250 differential calorimeter (TA Instruments), using hermetic aluminum pans, indium standard for calibration, nitrogen as the purge gas, a sample weight of about 5 mg. The sample was heated up to 200 °C at a heating rate of 20 °C/min, followed by an isotherm at 200 °C for 2 min and cooling to −40 °C at a cooling rate of 10 °C/min. Then, the second heating process was carried out from −40 to 200 °C at a heating rate of 10 °C/min, followed by an isotherm at 200 °C for 2 min. Thermogravimetric analysis (TGA) was performed on a TGA2 instrument from Mettler Toledo. Around 5 mg of the sample was heated to 600 °C at 20 °C/min under N_2 (20 mL/min). X-ray diffractograms of the samples placed on a zero-background plate were collected using a Bruker D8 TWIN−TWIN diffractometer in the Bragg−Brentano configuration (Cu Kα radiation, 0.02° step size). Swelling tests were carried out with round disc-shaped specimens. The latter was immersed in ethanol for 24 h at 25 °C (until the equilibrium was reached). Subsequently, the swollen samples were weighted and then dried overnight under vacuum at 40 °C to obtain the dry weight. The swelling percentage was defined as the weight ratio ($[(W_s - W_d)/W_d] \times 100$), where W_s is the weight of gel in the swollen state at equilibrium and W_d is the weight of gel in the dry state. Three measurements were carried out, and the reported swelling percentage is the average value. Shear rheological experiments were performed on a rotational rheometer (ARES-G2) equipped with parallel-plate geometry (diameter of 8 mm) and heat exchanger. Gaps of 0.6−0.7 mm were set to minimize edge fracture effects and ensure a reasonable aspect ratio of plate radius and gap so that the geometry was completely filled. Normal forces were monitored to be relaxed prior any measurement. Dynamic frequency sweep experiments were performed. To do so, small amplitude frequency sweep (SAOS) tests were carried out under strain control at angular frequencies in the range of 1−100 rad/s, with a strain of 1% and at a constant temperature of 25 °C in an ethanol-saturated atmosphere in order to minimize evaporation of the solvent.

Synthesis of 4,4-Dimethyl-5-methyleneoxazolidinone (DMOx). 1,1-Dimethyl-prop-2-ynylamine (8.7 g, 104.7 mmol) and $AgNO_3$ (0.089 g, 0.52 mmol) were dissolved in degassed dimethyl sulfoxide (DMSO) (11 mL) and heated at 30 °C under 15 bar of CO_2 during 4 h. After cooling the reaction mixture to room temperature, the mixture was extracted by $CHCl_3$/H_2O and the organic phase (dried over $MgSO_4$) was purified by column chromatography [hexane/ethyl acetate: 4/1 (v/v)]. The crude product was further purified by recrystallization by hexane and ethyl acetate [hexane/ethyl acetate: 4/1 (v/v)]. DMOx was

Published in : Macromolecules (2021), vol.54, n°22, pp. 10415–10427
DOI: 10.1021/acs.macromol.1c01895
Status : Postprint (Author's version)

collected as white crystals (10 g) in 75% yield. ^{1}H NMR ($CDCl_3$): δ 6.92 (s, 1H, NH), 4.63 (d, J = 3.4 Hz, 1H, −C=CH_2), 4.21 (d, J = 3.3 Hz, 1H, −C=CH_2), 1.45 (s, 6H, −CH_3). ^{13}C{^{1}H} NMR ($CDCl_3$): δ 162.22 (C=O), 155.75 (−O−C=CH_2), 84.23 (−O−C=CH_2), 58.40 (−$C(CH_3)_2$), 29.37 (−CH_3). FTIR (cm^{-1}): 3159 (NH), 2973 (CH_3), 1748 (N−C=O), 1708 (O−C=O), 1668 (C=CH_2).

Conventional Radical Copolymerization of VAc and Ethylene. V-70 (1.67 g, 5.40 mmol) was placed in a 25 mL Schlenk tube under argon. After the addition of degassed VAc (16.59 mL, 15.50 g, 180 mmol), the solution was transferred to a previously purged 30 mL stainless-steel autoclave under mild ethylene flux. After closing the reactor, the pressure of ethylene was then increased to 50 bar and polymerization was carried out at 40 °C. After 24 h, samples were withdrawn for NMR and SEC analyses to determine conversions and the molecular parameters of the polymer, respectively. The final copolymer was purified by repeated precipitations in hexane, followed by drying under vacuum at 60 °C overnight before characterization by ^{1}H NMR, ^{13}C{ ^{1}H} NMR, HSQC, and COSY in DMSO-d_6. A similar experiment was carried out under 25 bar of ethylene, keeping constant all other parameters ($[VAc]_0/[initiator]_0$ = 100/3).

Conventional Radical Terpolymerization of DMOx, VAc, and Ethylene. AIBN (0.12 g, 0.75 mmol) and DMOx (0.64 g, 5 mmol) were placed in a 15 mL Schlenk tube under argon. After the addition of degassed VAc (1.84 mL, 1.72 g, 20 mmol), the solution was transferred to a previously purged 30 mL stainless-steel autoclave under mild ethylene flux. The reactor was closed, the pressure of ethylene was then increased to 50 bar, and polymerization was carried out at 65 °C. After 24 h, samples were withdrawn for NMR and SEC analyses to determine conversions and the molecular parameters of the polymer, respectively. The final copolymer was purified by precipitations in diethyl ether three times followed by drying under vacuum at 60 °C overnight before characterization by ^{1}H NMR,^{13}C{ ^{1}H} NMR, HSQC, and COSY in DMSO-d_6.

A similar experiment was carried out with V-70 at 40 °C, keeping constant all other parameters, ($[VAc]_0/[DMOx]_0/[initiator]_0$ = 80/ 20/3, 50 bar of ethylene).

A similar experiment was also carried out with different initial comonomer feed ratios ($[VAc]_0/[DMOx]_0/[AIBN]_0$ = 60/40/3) using AIBN as the initiator at 65 °C, keeping constant all other parameters.

Conventional Radical Copolymerization of DMOx and Ethylene. AIBN (0.049 g, 0.3 mmol) and DMOx (1.27 g, 10 mmol) were placed in a 15 mL Schlenk tube under argon. After the addition of degassed DMC (5 mL), the solution was transferred to a previously purged 30 mL stainless-steel autoclave under mild ethylene flux. The reactor was closed, the pressure of ethylene was then increased to 50 bar, and polymerization was carried out at 65 °C. After 24 h, samples were withdrawn for NMR and SEC analyses to determine conversions and the molecular parameters of the polymer, respectively. The final copolymer was purified by precipitations in diethyl ether three times followed by drying under vacuum at 60 °C overnight before characterization by ^{1}H NMR, ^{13}C{^{1}H} NMR, HSQC, and COSY in DMSO-d_6.

A similar experiment was carried out with different monomer initiator ratios ($[DMOx]_0/[AIBN]_0$ = 100/10), keeping constant all other parameters.

A similar experiment was carried out in bulk with different monomer initiator ratios ($[DMOx]_0/[AIBN]_0$ = 100/10) at 80 °C, keeping constant all other parameters.

Published in : Macromolecules (2021), vol.54, n°22, pp. 10415–10427
DOI: 10.1021/acs.macromol.1c01895
Status : Postprint (Author's version)

Organometallic-Mediated Radical Copolymerization of DMOx, VAc, and Ethylene. DMOx (1.27 g, 10 mmol) was placed in a 15 mL Schlenk tube under argon. A solution of alkyl-cobalt(III) initiator ($PVAc_{<4}$-$Co(acac)_2$) in CH_2Cl_2 (2.3 mL of a 0.086 M stock solution, 0.2 mmol) was added into the same Schlenk tube followed by evaporation of CH_2Cl_2 under reduced pressure at room temperature. Then, degassed VAc (3.68 mL, 3.40 g, 40 mmol) was injected under argon. The reaction mixture ($f°_{DMOx}$ = 0.2 and $f°_{VAc}$ = 0.8, $[VAc]_0/[DMOx]_0/[PVAc_{<4}\text{-}Co(acac)_2]_0$ = 200/50/1) was then transferred to a previously purged 30 mL stainless-steel autoclave under mild ethylene flux. The reactor was closed, the pressure of ethylene was then increased to 50 bar, and polymerization was carried out at 50 °C. During polymerization, samples were regularly taken and TEMPO was added to the samples in order to quench the polymerization. The conversion of VAc and DMOx was determined by ^{1}H NMR in DMSO-d_6 (1 mg of TEMPO was added per mL of DMSO-d_6). The molecular parameters (M_n and $Đ$) of the polymer were determined by SEC in DMF containing 0.025 M LiBr (samples were dissolved in DMF containing 10 mg of TEMPO/mL). Polystyrene was used as calibration. After 24 h, the polymerization mixture was quenched by the addition of 0.5 mL of TEMPO in DMSO (0.20 g/mL). The final copolymer was purified by precipitation in diethyl ether three times followed by drying at 60 °C overnight before characterization by ^{1}H NMR, $^{13}C\{^1H\}$ NMR, HSQC, and COSY in DMSO-d_6.

A similar experiment was carried out with different initial comonomer feed ratios ($f°_{DMOx}$ = 0.4 and $f°_{VAc}$ = 0.6, $[VAc]_0/[DMOx]_0/[PVAc_{<4}\text{-}Co(acac)_2]_0$ = 150/100/1), keeping constant all other parameters.

Organometallic-Mediated Radical Polymerization of DMOx and Ethylene. DMOx (0.64 g, 5 mmol) was placed in a 15 mL Schlenk tube under argon. A solution of alkyl-cobalt(III) initiator ($PVAc_{<4}$-$Co(acac)_2$) in CH_2Cl_2 (0.23 mL of a 0.086 M stock solution, 0.02 mmol) was added into the same Schlenk tube followed by evaporation of CH_2Cl_2 under reduced pressure at room temperature. Then, degassed DMC (2.5 mL) was injected under argon. The reaction mixture ($[DMOx]_0/[PVAc_{<4}\text{-}Co(acac)_2]_0$ = 250/1) was then transferred to a previously purged 30 mL stainless-steel autoclave under mild ethylene flux. The reactor was closed, the pressure of ethylene was then increased to 50 bar, and polymerization was carried out at 50 °C. During polymerization, samples were regularly taken and TEMPO was added to the samples in order to quench the polymerization. The monomer conversion was determined by ^{1}H NMR in DMSO-d_6 (1 mg of TEMPO was added per mL of DMSO-d_6). The molecular parameters (M_n and $Đ$) of the polymer were determined by SEC in DMF containing 0.025 M LiBr (samples were dissolved in DMF containing 10 mg of TEMPO/mL). The polystyrene was used as calibration. After 24 h, the polymerization mixture was quenched by the addition of 0.5 mL of TEMPO in DMSO (0.20 g/mL). The final copolymer was purified by precipitation in diethyl ether three times followed by drying at 60 °C overnight before characterization via ^{1}H NMR, $^{13}C\{^1H\}$ NMR, HSQC, and COSY in DMSO-d_6.

Synthesis of EVOH. EVA (8 g) was dissolved in MeOH (40 mL). NaOH (8 g, 0.2 mol) in deionized water (30 mL) was added to the reaction mixture followed by stirring at room temperature in a round-bottomed flask for 48 h. Subsequently, MeOH was evaporated, and EVOH precipitated out of the solution. The EVOH was collected and washed three times with deionized water and then dried under vacuum at 60 °C. EVOH was recovered as a white powder and characterized via ^{1}H NMR, $^{13}C\{^1H\}$ NMR, and HSQC in DMSO-d_6 and FTIR.

Synthesis of P(E-*co*-VOH-*co*-AMBO). P(E-co-VAc-*co*-DMOx) (3 g) was dissolved in MeOH (7 mL) followed by the addition of a NaOH aqueous solution (3 g of NaOH in 7 mL of deionized water). The

Published in : Macromolecules (2021), vol.54, n°22, pp. 10415–10427
DOI: 10.1021/acs.macromol.1c01895
Status : Postprint (Author's version)

reaction mixture was placed in a stainless-steel Parr bomb reactor and heated at 120 °C. After 48 h, the system was cooled to room temperature and added by MeOH (10 mL). The precipitated base was removed by filtration. The copolymer solution was dialyzed (membrane 1 kDa) against distilled water for 10 h in order to remove the residual base followed by dialysis against MeOH for 5 h. This operation was repeated two times. After evaporation of the solvent, the P(E-*co*-VOH-*co*-AMBO) copolymer was recovered as a powder and characterized by ^{1}H NMR, ^{13}C{^{1}H} NMR, and HSQC in DMSO-d_6 and FTIR.

Synthesis of P(E-*co*-VOH-*co*-POx). P($E_{0.30}$-*co*-$VOH_{0.46}$-*co*-$AMBO_{0.24}$) (50 mg) and hexanal (25 mg, 0.25 mmol, stoichiometric ratio of NH_2/HC=O) were dissolved in EtOH (0.63 mL) followed by stirring at room temperature in a round-bottomed flask for 24 h. The desired P($E_{0.30}$-*co*-$VOH_{0.46}$-*co*-$POx_{0.24}$) copolymer was purified by precipitation in distilled water three times followed by drying at 60 °C under vacuum overnight before characterization via ^{1}H NMR, ^{13}C{^{1}H} NMR, HSQC, and COSY in DMSO-d_6 and FTIR.

Acid Treatment of P(E-*co*-VOH-*co*-POx). P($E_{0.30}$-*co*-$VOH_{0.46}$-co-$POx_{0.24}$) (40 mg) was dissolved in MeOH (1.5 mL) in a round-bottomed flask and added with HCl·H_2O (37 wt %, 0.13 g). After stirring for 4 h at room temperature, 1 mL of distilled water was added to the solution followed by overnight stirring. Subsequently, the solution was dialyzed (membrane 1 kDa) in distilled water for 24 h before the addition of NaOH aqueous solution (5 M) and adjustment of pH at 10. Finally, the hydrolyzed polymer was collected by filtration and dried at 60 °C under vacuum overnight.

Synthesis of EVOH Networks. P($E_{0.30}$-*co*-$VOH_{0.46}$-*co*-$AMBO_{0.24}$) (0.2 g) was dissolved in EtOH (1.25 mL) in a 10 mL glass tube with a lid followed by shaking at room temperature using a microplate shaker (VWR) at 200 rpm. After the addition of glutaraldehyde (35 mg, 0.35 mmol, NH_2/HCO = 1/0.7 ratio), the solution was gently shaken for 15 min. The sample was then allowed to stand overnight leading to the formation of a cross-linked EVOH gel. The latter was dried under vacuum and the resulting network was characterized by solid-state NMR.

Table 1. Conventional Radical Copolymerization of Ethylene, Vac, and DMOx.

						conv. (%)[a]						
entry	init.	T (°C)	E (bar)	f°_{VAc}	f°_{DMOx}	VAc	DMOx	$M_{n,SEC}$ (g/mol)[b]	$Đ$[b]	F_E[c]	F_{VAc}[c]	F_{DMOx}[c]
1	V70	40	25	1	0	88		25 500	1.82	0.31	0.69	
2	V70	40	50	1	0	66		18 200	1.86	0.50	0.50	
3	V70	40	50	0.8	0.2	19	12	7000	1.72	0.37	0.53	0.10
4	AIBN	65	50	0.8	0.2	84	41	28 000	1.83	0.34	0.55	0.11
5	AIBN	65	50	0.6	0.4	86	55	24 000	1.76	0.30	0.46	0.24
6[d]	AIBN	65	50	0	1		4	5000	1.34	0.77		0.23
7[d]	AIBN[e]	65	50	0	1		23	5100	1.63	0.74		0.26
8	AIBN[e]	80	50	0	1		12	2200	1.20	0.68		0.32

Conditions: 3 mol % of initiator compared to the monomers (entries 1–6). [a]Determined by ^{1}H NMR in DMSO-d_6. [b]Determined by SEC in DMF/LiBr using PS calibration. [c]Determined by ^{1}H NMR in DMSO-d_6 after purification. [d]Polymerization performed in DMC (DMOx 2 M in DMC). [e]10 mol % of AIBN compared to the monomers.

Published in : Macromolecules (2021), vol.54, n°22, pp. 10415–10427
DOI: 10.1021/acs.macromol.1c01895
Status : Postprint (Author's version)

Results and Discussion

Oxazolidinone-Functional EVAs and PEs via Conventional Radical Copolymerization. In the last decades, the use of CO_2 as a renewable feedstock has received a lot of interest for the synthesis of functional molecules and polymers. This abundant building block notably served for the preparation of 4,4-dimethyl-5-methyleneoxazolidin-2-one (DMOx)[48,51,52] used herein for the functionalization of EVAs and EVOHs. Inspired by previous reports,[48,51,52] DMOx was obtained in excellent yields by carboxylative cyclization of 1,1dimethyl-prop-2-ynylamine catalyzed by $AgNO_3$ at 30 °C under 15 bar of CO_2.

Before considering the synthesis of the oxazolidinone-containing copolymers, we prepared EVA precursors with different compositions as reference materials. These EVAs were synthesized via E/VAc copolymerizations initiated by a low-temperature radical initiator, namely, V-70, in the bulk at 40 °C. The content of ethylene in the copolymer was tuned from 31 to 50 mol % by working at 25 or 50 bar of ethylene pressure, respectively (**Table 1** entries 1 and 2). The EVAs' composition was determined by ^{1}H NMR (**Figure S1**). These temperature and pressure conditions (40 °C and 50 bar) were then applied to the terpolymerization of ethylene with VAc and DMOx ($[VAc]_0/[DMOx]_0 = 0.8/0.2$) (**Table 1**, entry 3). After 24 h, however, the monomer conversion remained low (<20%) with the formation of a terpolymer of moderate molar mass (7000 g/mol). By performing the same experiment at a higher temperature (65 °C) using AIBN as the initiator, decent monomer conversions were obtained (84 and 41% for VAc and DMOx, respectively) and the copolymer molar mass was significantly increased (28 000 g/mol) (**Table 1** entry 4). Besides typical signals of EVAs, characteristic peaks of DMOx units appeared in the ^{1}H NMR, HSQC (**Figure 1**), and COSY (**Figure S2**) spectra. The copolymer composition was determined by comparing the intensity of signal c corresponding to −CH− of VAc units at 4.8 ppm and signal g assigned to −NH− of DMOx at 7.5 ppm with signals between 1 and 2 ppm containing peaks a of $-CH_2-$ of ethylene units as well as methyl and methylene groups of VAc and DMOx. The molar fraction of DMOx in the terpolymer was evaluated at 0.11, whereas the E and VAc molar fractions reached 0.34 and 0.55, respectively. The E/VAc/DMOx copolymerization was then carried out under 50 bar of ethylene at 65 °C with a higher DMOx content in the feed ($[VAc]_0/[DMOx]_0 = 0.6/0.4$) (**Table 1** entry 5). Based on the NMR characterization (**Figure S3**), the DMOx content in the P(E-*co*-VAc-*co*-DMOx) terpolymer was increased to 24 mol % while preserving an ethylene content of 30 mol %.

Next, the ethylene/DMOx copolymerization was investigated at 65 °C under 50 bar of ethylene using 3 mol % AIBN (**Table 1**, entry 6). Since DMOx is a solid with a melting point of about 69 °C, the E/DMOx copolymerization was performed in DMC, a solvent known for its low transfer constant in ethylene polymerizations.[53] After 24 h, a P(E-co-DMOx) copolymer with a moderate molar mass (5000 g/mol) and DMOx content of 23 mol % was collected. However, the DMOx conversion did not exceed 4%. Increasing the amount of AIBN from 3 to 10 mol % at 65 °C increased the DMOx conversion to 23% without affecting the molar mass and the composition of the copolymer (**Table 1** entry 7). Typical ^{1}H NMR, HSQC, and COSY spectra of the P(E-co-DMOx) copolymer are shown in **Figures 2** and **S4**. Finally, the E/ DMOx copolymerization was tested in bulk at 80 °C, so above the melting temperature of DMOx, no improvement of the conversion and molar mass was observed (**Table 1** entry 8). Overall, conventional radical copolymerization gave access to a series of DMOx-containing EVAs and PE with DMOx content up to 25 mol % and dispersity ranging from 1.5 to 2.

Published in : Macromolecules (2021), vol.54, n°22, pp. 10415–10427
DOI: 10.1021/acs.macromol.1c01895
Status : Postprint (Author's version)

Oxazolidinone-Functional EVAs and PEs by RDRP. The reversible deactivation radical copolymerization of DMOx with ethylene and VAc was then investigated in order to produce P(E-*co*-VAc-*co*-DMOx) and P(E-*co*-DMOx) copolymers with predictable molar mass, low dispersity, and precise composition. For this purpose, we considered the organometallic-mediated radical polymerization (OMRP),[54–57] an efficient RDRP technique for controlling the polymerization of many less-activated monomers[55,58] as well as the ethylene/VAc[59–61] and VAc/DMOx[48] copolymerizations. These copolymerizations were typically initiated by an alkyl-cobalt initiator, that is, PVAc$_{\sim 4}$-Co(acac)$_2$,[50] at 40−50 °C which is the optimal temperature range for the OMRP process involving such Co(acac)$_2$-carbon bonds.

On this basis, the controlled radical terpolymerization of ethylene, VAc, and DMOx was tested at 50 °C under 50 bar of ethylene in bulk using the alkyl-Co(acac)$_2$ initiator (**Scheme 2**, **Table 2** entries 1 and 2). Two initial VAc/DMOx feed ratios were considered, namely, an f °$_{DMOx}$ of 0.2 and 0.4 (**Table 2** entries 1 and 2). Molecular parameters (M_n and $Đ$) of the copolymer and monomer conversion were monitored throughout the polymerization by SEC and ^{1}H NMR, respectively. In both cases, the molar mass of P(E-*co*-VAc-*co*-DMOx) increased regularly with the comonomer conversion as indicated by **Figure 3** and the overlay of the SEC chromatograms (**Figure S5**), suggesting the controlled character of the copolymerization. Moreover, the dispersity remained low throughout the polymerization, however, broadened around 50% conversion certainly due to some irreversible termination reactions. This phenomenon may result from the difference in reactivity between VAc and DMOx. Indeed, considering the individual conversions of the comonomers, VAc is preferentially consumed over DMOx at the early stage of the reaction, leading to the accumulation of DMOx in the feed which seems detrimental to the control of the terpolymerization. Nevertheless, the controlled copolymerization of E/VAc/DMOx was achieved by OMRP under mild temperature and pressure conditions and the resulting terpolymers were characterized by ^{1}H- and 2D NMR (**Figure S6**). Expectedly, the molar fraction of DMOx in the terpolymer increased from 0.15 to 0.25 when increasing the DMOx content in the feed (f°$_{DMOx}$) from 0.2 to 0.4, suggesting a possible control of the oxazolidinone content in the EVA-DMOx copolymer (compare **Table 2** entries 1 and 2).

Finally, the OMRP of E/DMOx copolymerization was tested under similar temperature and pressure (50 °C, 50 bar) using DMC as a solvent (**Table 2**, entry 3). Although polymerization was slow and the conversion only reached 16% after 24 h, the M_n of P(E-*co*-DMOx) clearly increased regularly with the monomer conversion with a low-to-moderate dispersity ($Đ$ ∼1.13−1.50). At the term of the polymerization, a P(E-*co*-DMOx) copolymer (7900 g/mol) containing 24 mol % DMOx was obtained.

Published in : Macromolecules (2021), vol.54, n°22, pp. 10415–10427
DOI: 10.1021/acs.macromol.1c01895
Status : Postprint (Author's version)

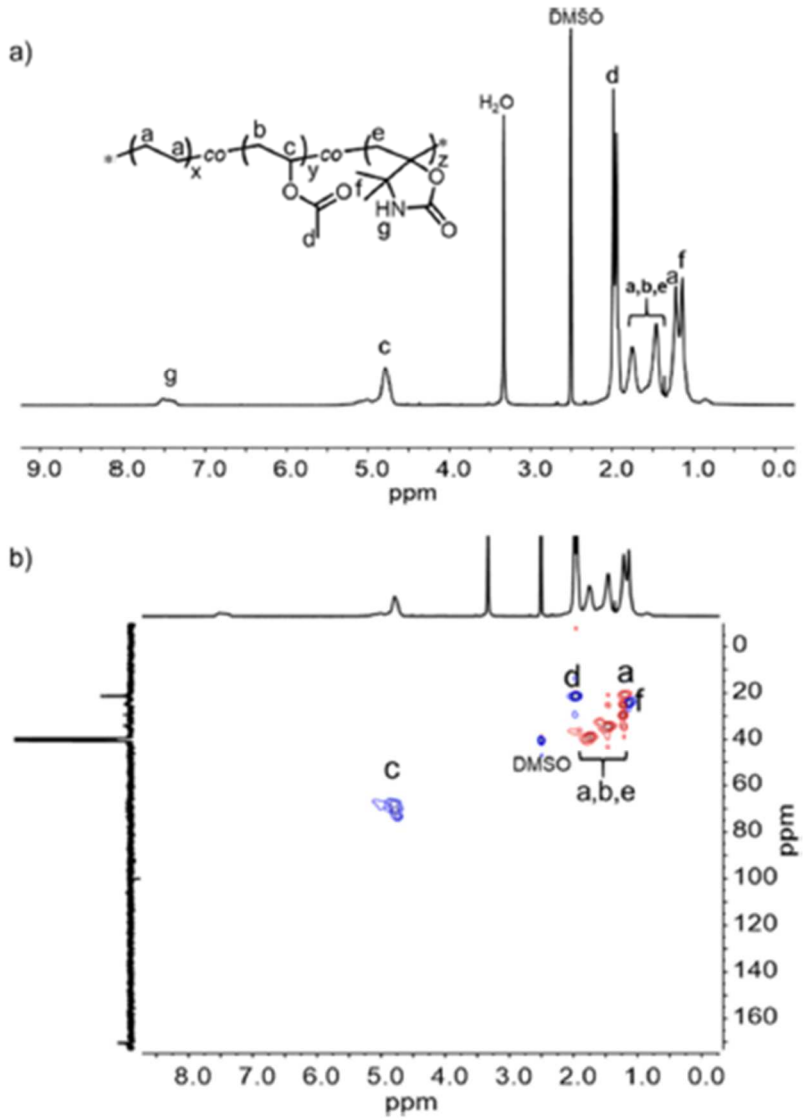

Figure 1. ^{1}H NMR (a) and HSQC (b) spectra in DMSO-d_6 of P($E_{0.34}$-*co*-$Vac_{0.55}$-*co*-$DMOx_{0.11}$) prepared by conventional radical polymerization (**Table 1**, entry 4).

Published in : Macromolecules (2021), vol.54, n°22, pp. 10415–10427
DOI: 10.1021/acs.macromol.1c01895
Status : Postprint (Author's version)

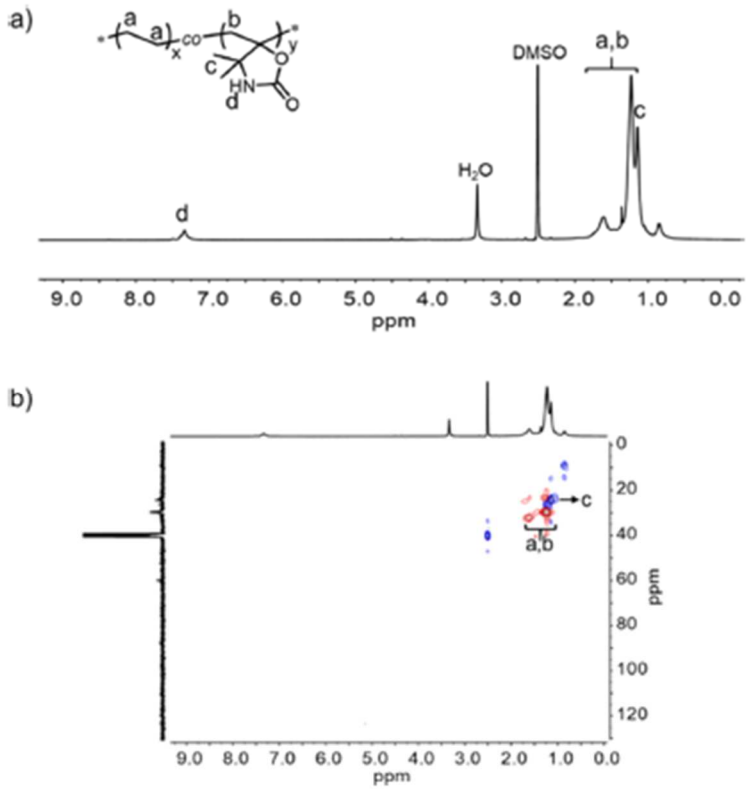

Figure 2. ^{1}H NMR (a) and HSQC (b) spectra in DMSO-d_6 of P(E0.74-*co*-DMOx$_{0.26}$) prepared by conventional radical polymerization (**Table 1**, entry 7).

Scheme 2. Organometallic-Mediated Radical Copolymerization of Ethylene, VAc, and DMOx.

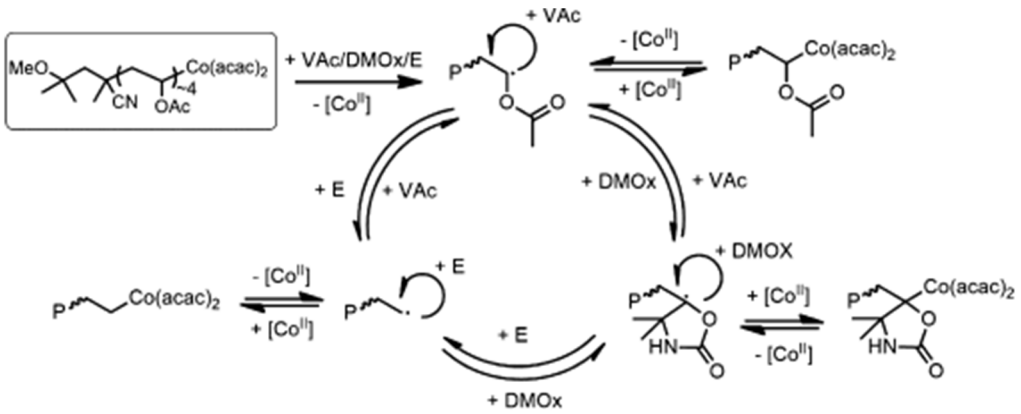

Published in : Macromolecules (2021), vol.54, n°22, pp. 10415–10427
DOI: 10.1021/acs.macromol.1c01895
Status : Postprint (Author's version)

Table 2. Organometallic-Mediated Radical Copolymerization of E, Vac, and DMOx.

					conv. (%)[a]							
entry	E (bar)	f°_{VAc}	f°_{DMOx}	time (h)	VAc	DMOx	total	$M_{n\ SEC}$ (g/mol)[b]	$Đ$[b]	F_E[c]	F_{VAc}[c]	F_{DMOx}[c]
1	50	0.8	0.2	1	2	1	5	3500	1.08			
				2	6	3	10	5400	1.08			
				3	12	4	15	6900	1.12			
				4	26	6	20	7900	1.16			
				5	37	8	27	9000	1.19			
				23	70	19	60	14 800	1.54	0.31	0.54	0.15
2	50	0.6	0.4	1	7	0	4	3500	1.07			
				2	9	5	7	5600	1.11			
				3	14	7	11	6800	1.13			
				4	22	11	18	7900	1.17			
				5	26	13	21	9100	1.21			
				6	32	15	25	10 000	1.22			
				22	56	20	42	14 500	1.53	0.33	0.42	0.25
3[d]	50		1.0	1		4	4	4600	1.13			
				2		5	5	5400	1.20			
				3		5	5	6700	1.22			
				4		6	6	7000	1.32			
				5		7	7	7500	1.38			
				22		16	16	7900	1.50	0.76		0.24

Conditions: 50 °C, 50 bar ethylene, [RCo]/[VAc and DMOx] = 1/250. [a]Determined by ^{1}H NMR in DMSO-d_6. [b]Determined by SEC in DMF/ LiBr using PS calibration. [c]Determined by ^{1}H NMR in DMSO-d_6 after purification. [d]Polymerization performed in DMC (DMOx 2 M in DMC).

Vicinal Amino-Alcohol-Functional EVOHs. 2-Oxazolidinones are widely used as protecting groups of 1,2-amino alcohols and regenerate the latter upon hydrolysis.[62−66] Therefore, we considered the modification of the DMOx-containing copolymers into novel vicinal amino alcohol-functional EVOHs.

The P(E-*co*-VAc-*co*-DMOx) terpolymer was transformed into the corresponding vicinal amino alcohol-functional EVOH, namely, P(E-*co*-VOH-*co*-AMBO), by hydrolysis in the presence of a strong base at high temperature (**Scheme 3**). To do so, P($E_{0.34}$-*co*-$VAc_{0.55}$-*co*-$DMOx_{0.11}$) (M_n = 28 000 g/mol) was reacted with sodium hydroxide in a MeOH/water mixture at 120 °C for 48 h (**Scheme 3**). Following this treatment, the formation of the desired P(E-*co*-VOH-*co*-AMBO) terpolymer was confirmed by FTIR notably through the appearance of intense and broad O−H and N−H stretching bands around 3300 cm^{-1}, the presence of a signal assigned to primary amines at 1588 cm^{-1}, and the disappearance of peaks corresponding to the oxazolidinone and ester moieties around 1730 cm^{-1} (**Figure 4a**). The quantitative conversion of P(E-*co*-VAc-*co*-DMOx) in its amino alcohol-containing EVOH counterparts was further proved by ^{1}H NMR (**Figure 4b**) as well as HSQC and COSY (**Figure S7**). Indeed, the ^{1}H signal c assigned to −C*H*− of VAc units shifted from 5.0 to 3.6 ppm, whereas the peak d assigned to −CH_3 of VAc units completely disappeared after this treatment, confirming the complete hydrolysis of VAc moieties. Moreover, the ^{1}H signal g assigned to −NH− of DMOx units at around 7.5 ppm fully disappeared and was replaced by a broad multiple peak between 4.12 and 4.88 ppm corresponding to the deprotected vicinal amino alcohol functions. The same hydrolytic procedure was successfully applied to the P($E_{0.30}$-*co*-$VAc_{0.46}$-*co*-$DMOx_{0.24}$) terpolymer with a higher oxazolidinone content (24 mol %) leading to an amino alcohol-rich EVOH derivative. However, the P($E_{0.74}$-*co*-$DMOx_{0.26}$) remained unchanged after a prolonged base treatment in a THF/water mixture at 120 °C.

Introducing these 1,2-amino alcohol functions along the EVOH backbone drastically changed its solution properties. In contrast to the conventional EVOHs whose solubilization requires solvents that

Published in : Macromolecules (2021), vol.54, n°22, pp. 10415–10427
DOI: 10.1021/acs.macromol.1c01895
Status : Postprint (Author's version)

are difficult to remove and unfavorable to the environment such as DMSO or DMF, P(E-*co*-VOH-*co*-AMBO)s completely dissolved in simple volatile alcoholic solvents such as MeOH and EtOH. These amino-containing EVOHs could also be dissolved in water at low pH and exhibited pH-responsiveness in water upon reversible protonation of their pendant amines, as shown in **Figure 5**. At pH 1, the amine groups of P(E-*co*-VOH-*co*-AMBO) are mainly in their protonated state, which favors the solubility of the terpolymer in water. Under these conditions, DLS revealed the presence of assemblies with a mean diameter of 760 nm that probably result from hydrophobic interactions between the ethylene-rich segments of the copolymer. After NaOH addition and deprotonation of the ammonium groups (pH 10), the P(E-*co*-VOH-*co*-AMBO) terpolymer immediately precipitated from water due to possible intermolecular H bonds involving amines and the loss of electrostatic repulsions between the chains (**Figure 5a**). This pH-triggered response was observed for several acidification/basification cycles, and the mean diameter of objects formed at pH 1 remained in the range of 750–850 nm (**Figure 5b**). To our knowledge, this amine-functionalizing method imparts pH-responsiveness to EVOH for the first time and offers new perspectives in the use of EVOHs in the field of metal chelation, construction of layer-by-layer, and chemical modifications, to name a few.

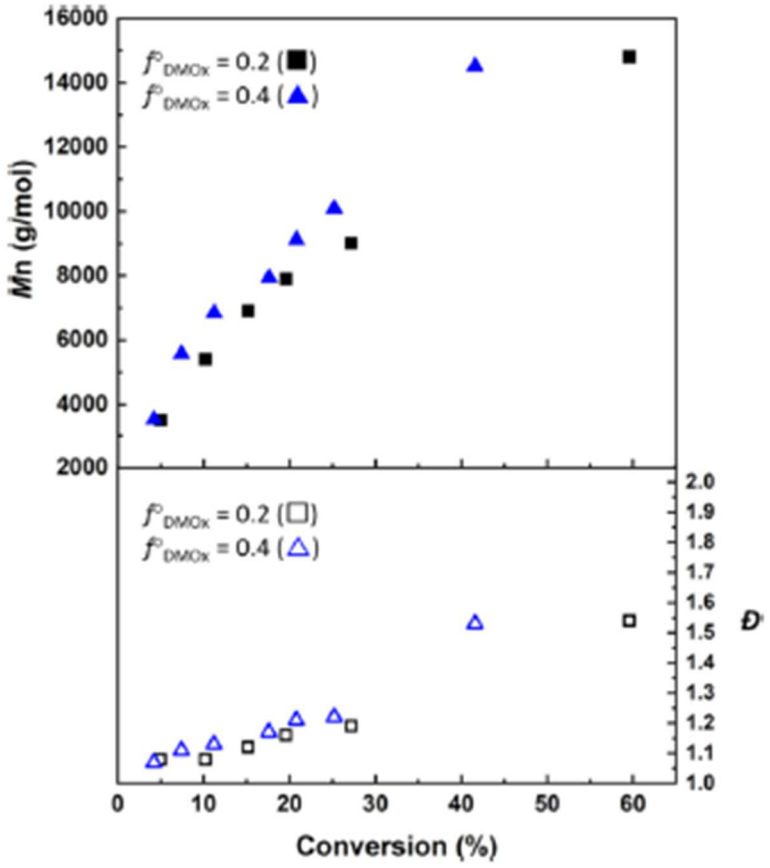

Figure 3. Dependence of M_n (full symbols) and $Đ$ (hollow symbols) on the total monomer (VAc and DMOx) conversion for the OMRP of E/VAc/DMOx with different compositions: f °$_{DMOx}$ = 0.2 (■) and 0.4 (blue ▲) (**Table 2**, entries 1 and 2).

Published in : Macromolecules (2021), vol.54, n°22, pp. 10415–10427
DOI: 10.1021/acs.macromol.1c01895
Status : Postprint (Author's version)

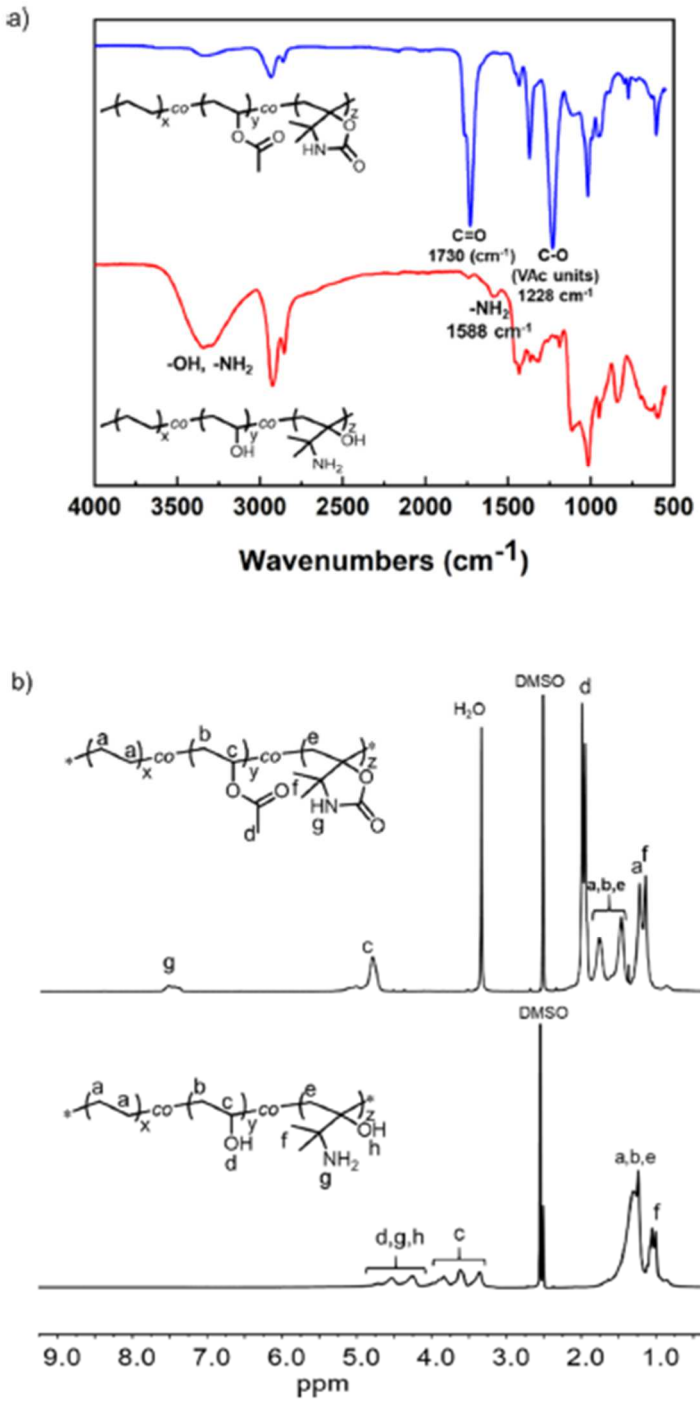

Figure 4. FTIR (a) and ^{1}H NMR in DMSO-d_6 spectra (b) of the P($E_{0.34}$-*co*-$VAc_{0.55}$-*co*-$DMOx_{0.11}$) (**Table 1**, entry 4) and the corresponding P($E_{0.34}$-*co*-$VOH_{0.55}$-*co*-$AMBO_{0.11}$) copolymer obtained by hydrolysis.

Oxazolidine-Functional EVOHs. 1,2-Amino alcohols exhibit a large variety of applications in chemical and pharmaceutical industries. In particular, their ability to condense with aldehydes is well-documented and gives access to 1,3-oxazolidines,[67,68] that is, heterocyclic structures present in several biologically active compounds.[69] These pH-sensitive molecules can be seen as cyclic acetal analogues with one oxygen atom replaced by nitrogen and notably served for the reversible protection of 1,2-

Published in : Macromolecules (2021), vol.54, n°22, pp. 10415–10427
DOI: 10.1021/acs.macromol.1c01895
Status : Postprint (Author's version)

amino alcohols.[70–72] In the light of these considerations, the conversion of the 1,2-amino alcohols of P(E-*co*-VOH-*co*-AMBO) into oxazolidines appeared as a method of choice for the selective and reversible post-modification of these amino-containing EVOH derivatives (**Scheme 4**).

First, the P($E_{0.30}$-*co*-$VOH_{0.46}$-*co*-$AMBO_{0.24}$) copolymer containing 24 mol % 1,2-amino alcohol functions was reacted with a low sterically hindered aldehyde, that is, hexanal, in ethanol with a stoichiometric NH_2/HC=O ratio at 25 °C for 24 h.

The quantitative formation of the desired 2-pentyl oxazolidine-functional EVOH, namely, P(E-*co*-VOH-*co*-POx), was confirmed by FTIR analysis (**Figure 6a**), ^{1}H NMR (**Figure 6b**), HSQC (**Figure 6c**), ^{13}C{^{1}H} NMR (**Figure S8a**), and COSY (**Figure S8b**). Indeed, the characteristic N−C*H*−O signal g of oxazolidine was detected at 4.4 and 4.4−88 ppm (δ^H–δ^C) in the ^{1}H NMR and HSQC spectra (**Figure 6b**,**c**), respectively. The latter also clearly evidenced the −CH_3 signal l of the lateral aliphatic chain. Based on the ^{13}C{^{1}H} NMR (**Figure S8a**) and HSQC (**Figure 6C**), we excluded the formation of imines and acetals via condensation of hexanal with the amines and 1,3-diols of P(E-*co*-VOH-*co*-AMBO), respectively. Indeed, no signal was detected around 160 ppm for the −N=CH− of imines and at 100 ppm for the O−C*H*−O of acetals. The absence of imines in the P(E-*co*-VOH-*co*-POx) sample was also confirmed by the lack of the −N=C*H*− signal at 6.5 ppm in ^{1}H NMR. Finally, the full consumption of the vicinal amino alcohol functions of P(E-*co*-VOH-*co*-AMBO) upon reaction with hexanal was further supported by the disappearance of the FTIR peak characteristic of primary amines of P(E-*co*-VOH-*co*-AMBO) at 1574 cm^{-1} (strong intensity) and 3350 cm^{-1} (shoulder peak) (**Figure 6a**).

Next, we tested the regeneration of the 1,2-amino alcohol functions via acidic hydrolysis of the oxazolidine groups of P(E-*co*-VOH-*co*-POx). To do so, P($E_{0.30}$-*co*-$VOH_{0.46}$-*co*-$POx_{0.24}$) was treated at room temperature in methanol added with concentrated HCl_{aq}. Following this, the primary amine FTIR peak reappeared at 1574 cm^{-1} confirming the release of amino-alcohol moieties (**Figure S9a**). As a confirmation, the ^{1}H NMR signals corresponding to the vicinal amino alcohols were detected between 4 and 5 ppm (**Figure S9b**). Nevertheless, the hydrolysis seemed partial (about 61% conversion) as assessed by the residual peak at 0.85 ppm assigned to −CH_3 of the aliphatic lateral chain of the oxazolidine (**Figure S9b**).

Finally, P($E_{0.30}$-*co*-$VOH_{0.46}$-*co*-$AMBO_{0.24}$) was reacted at room temperature in ethanol with a bis-aldehyde compound, namely, glutaraldehyde, to target EVOH networks by specific conversion of the amino alcohol functions into oxazolidines. Under these mild conditions, an EVOH gel swollen by ethanol was collected (**Figure 7a**). The network structure and selective formation of oxazolidine groups were demonstrated by ^{13}C solid-state NMR (**Figure 7b**). Again, no signals corresponding to the −N=CH− of imines and O−CH−O of acetals were detected at 160 and 100 ppm, respectively. Overall, the vicinal amino alcohol functions are converted into oxazolidine groups without the formation of acetals in contrast to the classical glutaraldehyde cross-linking process of VOH-containing polymers. Such a selective cross-linking reaction opens new perspectives in the field of networks, notably the possibility to control the distribution of the cross-linking points within a network composed of VOH units. As a preliminary characterization of this EVOH network, swelling experiments were carried out. For this purpose, samples were immersed in ethanol at ambient temperature for 24 h (until an equilibrium state was reached). After weighting and drying the samples, we measured a swelling percentage equal to 370%. In addition, the dynamic mechanical properties of this EVOH gel in ethanol were investigated

Published in : Macromolecules (2021), vol.54, n°22, pp. 10415–10427
DOI: 10.1021/acs.macromol.1c01895
Status : Postprint (Author's version)

under low-strain conditions by oscillatory shear characterized by an equilibrium in both storage (*G*') and loss (*G*") moduli under decreasing frequency (ω) (**Figure S10**). Typically, *G*' was about three times higher than *G*" in the investigated range which assessed the elastic and cross-linked character of the gel.

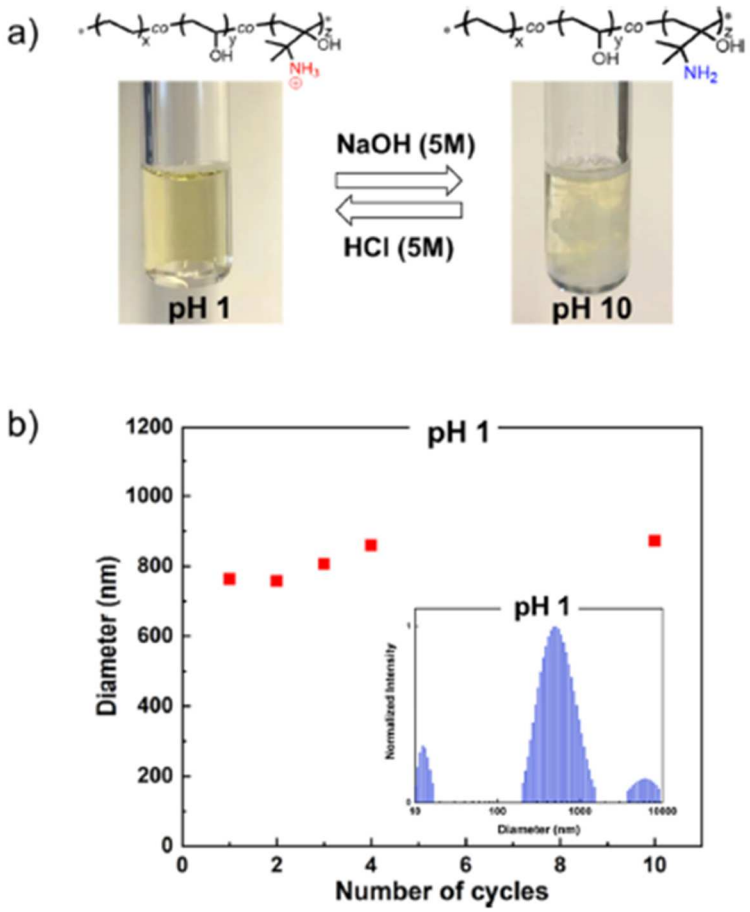

Figure 5. (a) pH-responsive behavior of P($E_{0.30}$-*co*-$VOH_{0.46}$-*co*-$AMBO_{0.24}$) in water (2.5 mg/mL). (b) Average DLS diameter of the objects formed by P($E_{0.30}$-*co*-$VOH_{0.46}$-*co*-$AMBO_{0.24}$) in water at pH 1 after a different number of acidification (pH 1)/basification (pH 10) cycles.

Published in : Macromolecules (2021), vol.54, n°22, pp. 10415–10427
DOI: 10.1021/acs.macromol.1c01895
Status : Postprint (Author's version)

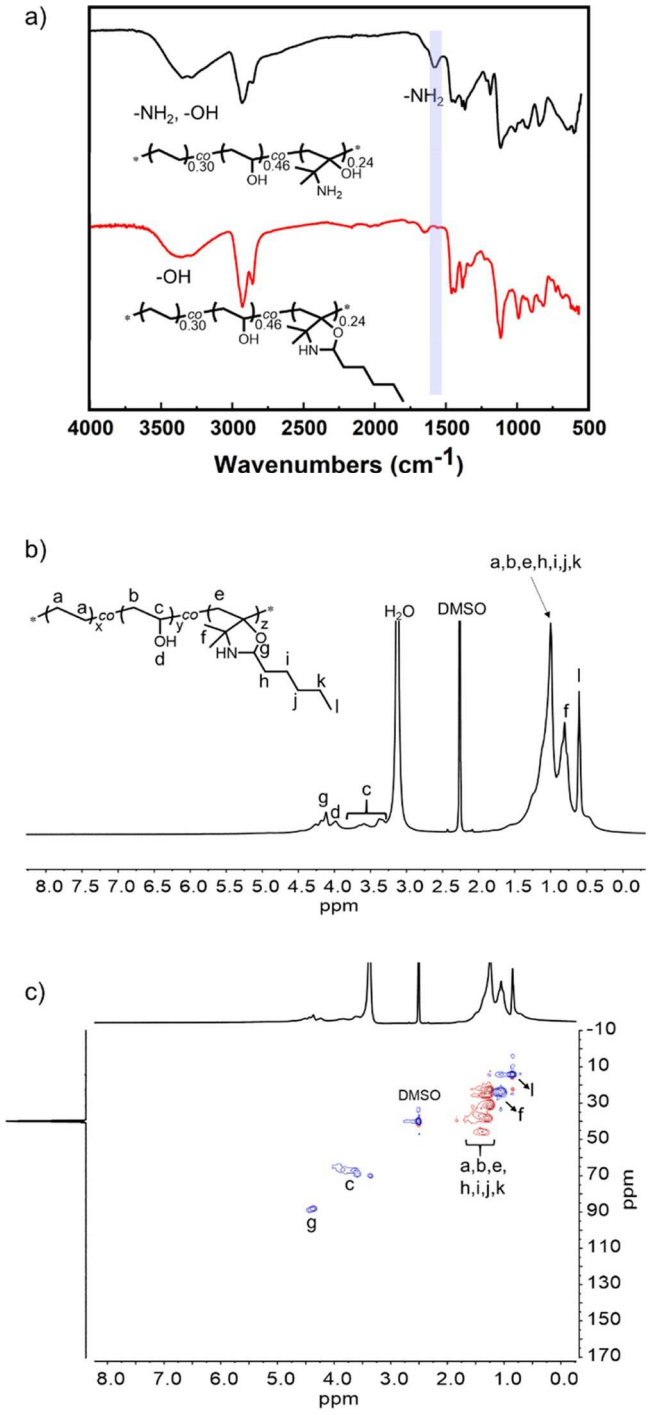

Figure 6. FTIR spectra (a) of the P($E_{0.30}$-*co*-$VOH_{0.46}$-*co*-$AMBO_{0.24}$) precursor (black) and P($E_{0.30}$-*co*-$VOH_{0.46}$-*co*-$POx_{0.24}$) resulting from condensation with hexanal (red). ^{1}H NMR (b) and HSQC (c) spectra of P($E_{0.30}$-*co*-$VOH_{0.46}$-*co*-$POx_{0.24}$) in DMSO-d_6.

Published in : Macromolecules (2021), vol.54, n°22, pp. 10415–10427
DOI: 10.1021/acs.macromol.1c01895
Status : Postprint (Author's version)

Scheme 4. Selective Post-modification of the 1,2-Amino Alcohol-Containing EVOHs via the Formation of 1,3-Oxazolidine Moieties

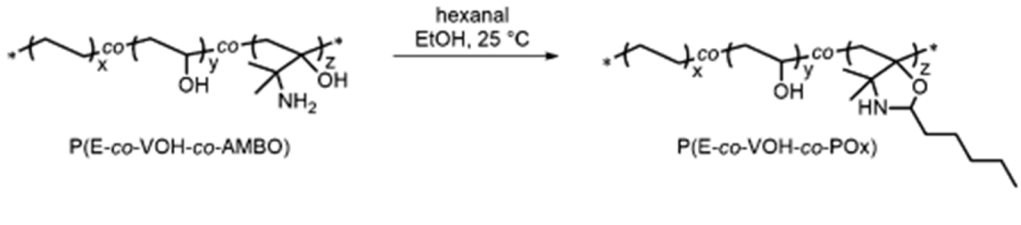

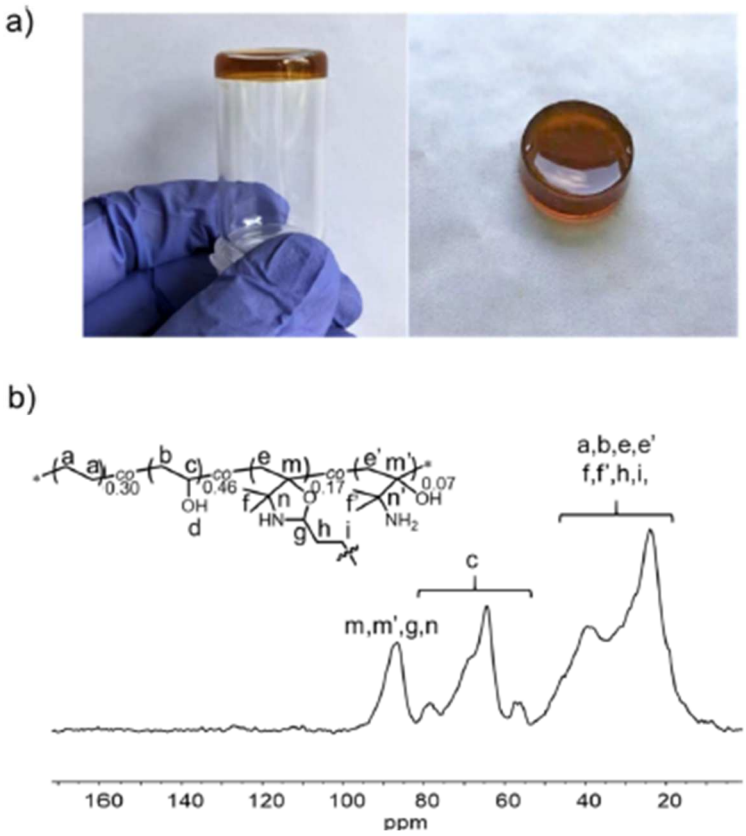

Figure 7. Gel formation upon cross-linking of P($E_{0.30}$-*co*-$VOH_{0.46}$-*co*-$AMBO_{0.24}$) with glutaraldehyde in ethanol (a) and ^{13}C solid-state NMR spectrum of the resulting EVOH network (b).

Thermal Properties of the Functional EVAs and EVOHs. As far as applications are concerned, the thermal properties of EVAs and EVOHs are of prime importance and strongly depend on their composition. Hereafter, we investigated the thermal behavior of the functional EVAs and EVOHs prepared in this study by DSC and TGA. Some EVAs and their corresponding EVOHs were used as references.

DSC curves of the EVAs and DMOx containing copolymers are presented in **Figure 8a**. Expectedly, due to a higher ethylene content, P($E_{0.5}$-*co*-$VAc_{0.5}$) showed a lower glass transition temperature (T_g = −3.3 °C) compared to P($E_{0.31}$-*co*-$VAc_{0.69}$) (T_g = 16.9 °C). Moreover, the incorporation of DMOx within the EVA backbone significantly increased its T_g. Indeed, for a similar ethylene molar fraction (around 0.3), P($E_{0.34}$-*co*-$VAc_{0.55}$-*co*-$DMOx_{0.11}$) and P($E_{0.30}$-*co*-$VAc_{0.46}$-*co*-$DMOx_{0.24}$) exhibited higher glass transition

Published in : Macromolecules (2021), vol.54, n°22, pp. 10415–10427
DOI: 10.1021/acs.macromol.1c01895
Status : Postprint (Author's version)

temperature (48.6 and 72.9 °C, respectively) compared to P($E_{0.31}$-*co*-$VAc_{0.69}$). This is explained by the insertion of rigid oxazolidinone rings along the backbone which restrict the mobility of the chains. Finally, the ethylene-rich P($E_{0.74}$-*co*-$DMOx_{0.26}$) showed a much higher T_g (66.3 °C) compared to P($E_{0.75}$-*co*-$VAc_{0.25}$) with a similar composition (T_g = −16 °C),[73] which further highlights the tendency of DMOx units to increase T_g. The thermal degradation of these functional polymers was also analyzed by TGA (**Figure S11a**). The EVAs and the DMOx-containing EVAs presented a two-step degradation profile characteristic of copolymers composed of VAc units. As reported for the classical EVAs,[74] the first step corresponds to the thermal degradation of the VAc functions via deacetylation. Moreover, the 5 wt % loss degradation temperature ($T_{deg\ 5\%}$) of P($E_{0.34}$-*co*-$VAc_{0.55}$-*co*-$DMOx_{0.11}$) was high and similar to P($E_{0.5}$-*co*-$VAc_{0.5}$) and P($E_{0.31}$-*co*-$VAc_{0.69}$) ($T_{deg\ 5\%}$ ~ 310 °C). However, a marked decrease in $T_{deg\ 5\%}$ occurred when the molar fraction of DMOx was increased to 0.24, $T_{deg\ 5\%}$ of P($E_{0.30}$-*co*-$VAc_{0.46}$-*co*-$DMOx_{0.24}$) = 231 °C. Deprived of VAc units, P($E_{0.74}$-*co*-$DMOx_{0.23}$) showed the highest thermal resistance with a remarkable $T_{deg\ 5\%}$ (372 °C). EVOH is a semicrystalline polymer whose T_g and T_m are known to increase with the content of vinyl alcohol. As an illustration, P($E_{0.31}$-*co*-$VOH_{0.69}$) (T_g = 63.5 °C, T_m = 190.4 °C) displayed higher transition temperatures compared to P($E_{0.5}$-*co*-$VOH_{0.5}$) (T_g = 48.6 °C, T_m = 158.5 °C) (**Figure 8b**). Because the hydrolysis of the oxazolidinone moieties releases amines and also alcohol functions mimicking the hydroxyl groups of EVOH, P($E_{0.34}$-*co*-$VOH_{0.55}$-*co*-$AMBO_{0.11}$) and P($E_{0.30}$-*co*-$VOH_{0.46}$-*co*-$AMBO_{0.24}$) contain approximatively the same amount of alcohol functions compared to P($E_{0.31}$-*co*-$VOH_{0.69}$) which thus constitutes a relevant reference material. First, the T_g of the copolymer increases in the order P($E_{0.31}$-*co*-$VOH_{0.69}$) < P($E_{0.34}$-*co*-$VOH_{0.55}$-*co*-$AMBO_{0.11}$) < P($E_{0.30}$-*co*-$VOH_{0.46}$-*co*-$AMBO_{0.24}$) (from 63.5 to 89.5 °C) certainly due to the amines which provide extra H-bonding sites and to the bulky side groups which hinder the chain motion. In contrast to P($E_{0.31}$-*co*-$VOH_{0.69}$), the DSC curves P($E_{0.34}$-*co*-$VOH_{0.55}$-*co*-$AMBO_{0.11}$) and P($E_{0.30}$-*co*-$VOH_{0.46}$-*co*-$AMBO_{0.24}$) did not show any melting transition below 200 °C. The amorphous character of the vicinal amino alcohol-EVOHs was confirmed by the broad bumps in their X-ray diffraction (XRD) patterns consistent with the absence of a long-range order (**Figure S12**). In this case, the packing and crystallization of the polymer chains is most probably hampered by the pendant isopropyl amine groups of AMBO units. Finally, the oxazolidine-containing P($E_{0.30}$-*co*-$VOH_{0.46}$-*co*-$POx_{0.24}$) copolymer showed a slightly lower T_g (67.2 °C) compared to its P($E_{0.30}$-*co*-$VOH_{0.46}$-*co*-$AMBO_{0.24}$) precursor (89.5 °C) (**Figure 8b**). The introduction of rigid oxazolidine rings, supposed to restrict the chain mobility and increase the T_g, was thus counterbalanced by the presence of flexible aliphatic chains on the oxazolidines and the consumption of the amino alcohol H-bonding sites. Finally, degradation temperatures ($T_{deg\ 5\%}$) of EVOHs and P(E-*co*-VOH-*co*-AMBO)s were recorded between 246 and 272 °C, whereas the oxazolidine-containing copolymer seemed slightly more sensitive to thermal degradation ($T_{deg\ 5\%}$ = 224 °C) (**Figure S11b**). As reported for classical EVOHs,[75] a major degradation product in the first degradation step is probably water, produced by elimination of the hydroxyl side group. However, an in-depth study would be necessary to unravel the thermal degradation mechanism of these novel vicinal amino alcohol-containing EVOHs.

Published in : Macromolecules (2021), vol.54, n°22, pp. 10415–10427
DOI: 10.1021/acs.macromol.1c01895
Status : Postprint (Author's version)

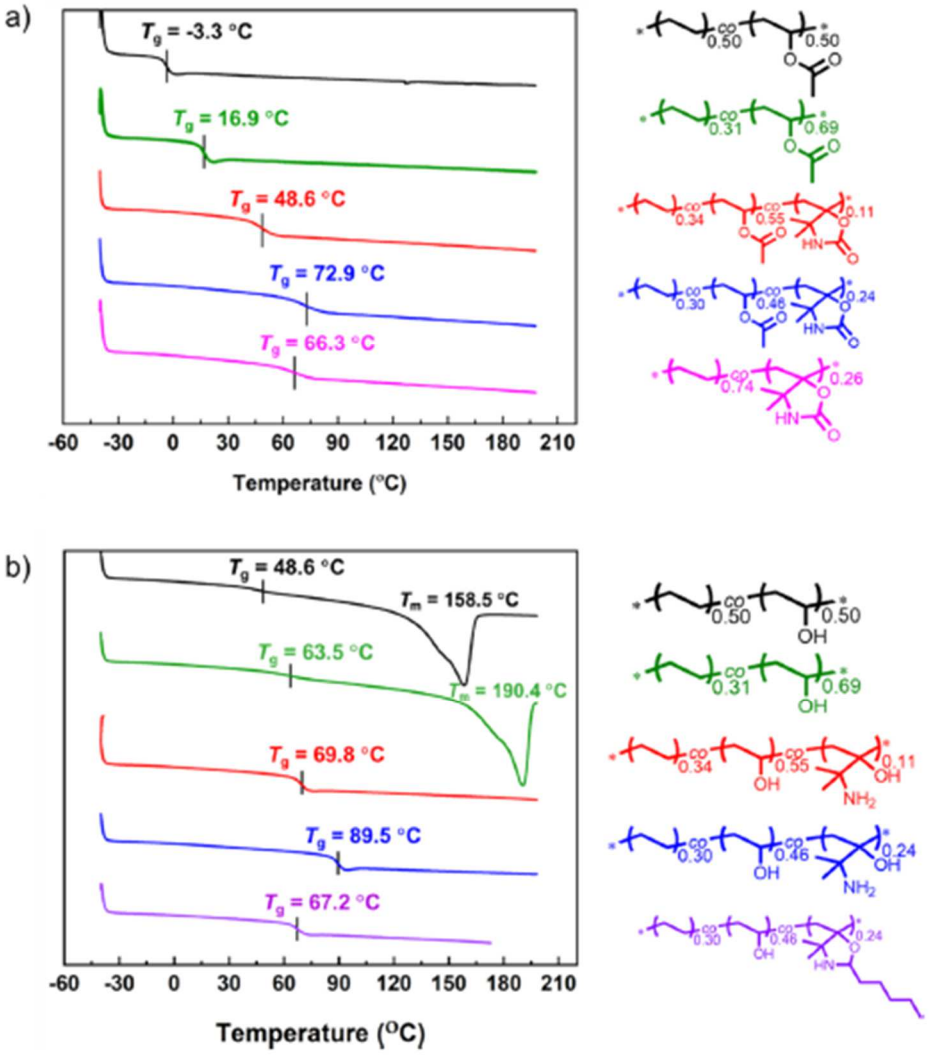

Figure 8. DSC curves of the EVA (a) and EVOH (b) derivatives.

Conclusions

In summary, we have described a straightforward synthesis platform for novel amino alcohol-functional EVOH copolymers. As a first step, a series of oxazolidinone-functionalized EVAs and PEs precursors were prepared via conventional radical copolymerization of ethylene and VAc with DMOx, an oxazolidinone-based methylene heterocycle derived from carbon dioxide. Copolymers with DMOx contents up to 25 mol % were synthesized. These copolymerizations were also successfully performed via reversible deactivation radical polymerization by OMRP giving access to the corresponding well-defined copolymers. The hydrolysis of the oxazolidinone-containing copolymers was then optimized under basic conditions to furnish unique vicinal amino alcohol-functional EVOHs. The incorporation of this peculiar motif along the EVOH chains not only improved their solubility but also imparted pH-responsiveness to EVOH samples for the first time and offered unique post-modification possibilities. As a proof of concept, the conversion of the pendant 1,2-amino alcohol groups into oxazolidines by

Published in : Macromolecules (2021), vol.54, n°22, pp. 10415–10427
DOI: 10.1021/acs.macromol.1c01895
Status : Postprint (Author's version)

reaction with an aldehyde was proved quantitative and selective, making this approach a tool of choice for modification of EVOHs. In this respect, EVOH gels were also successfully prepared by reacting the vicinal amino alcohol-containing polymers with a bis-aldehyde under mild conditions. Finally, the insertion of rigid oxazolidinone rings along the EVA backbone increased the glass transition of the latter, whereas the presence of 1,2-amino alcohols within the EVOH sample increased its glass transition and rendered it amorphous and easily soluble in alcohols.

Considering the valuable properties of the amine functional polymers such as ability to protonate, metal chelation ability, enhanced surface adhesion, and the specific reactivity of vicinal amino alcohol, this new synthesis platform based on the oxazolidinone building block is opening many prospects in the use of functional EVOHs and more generally, in the preparation of novel functional ethylene-based copolymers that are currently not accessible by other techniques.

Associated Content

SUPPORTING INFORMATION

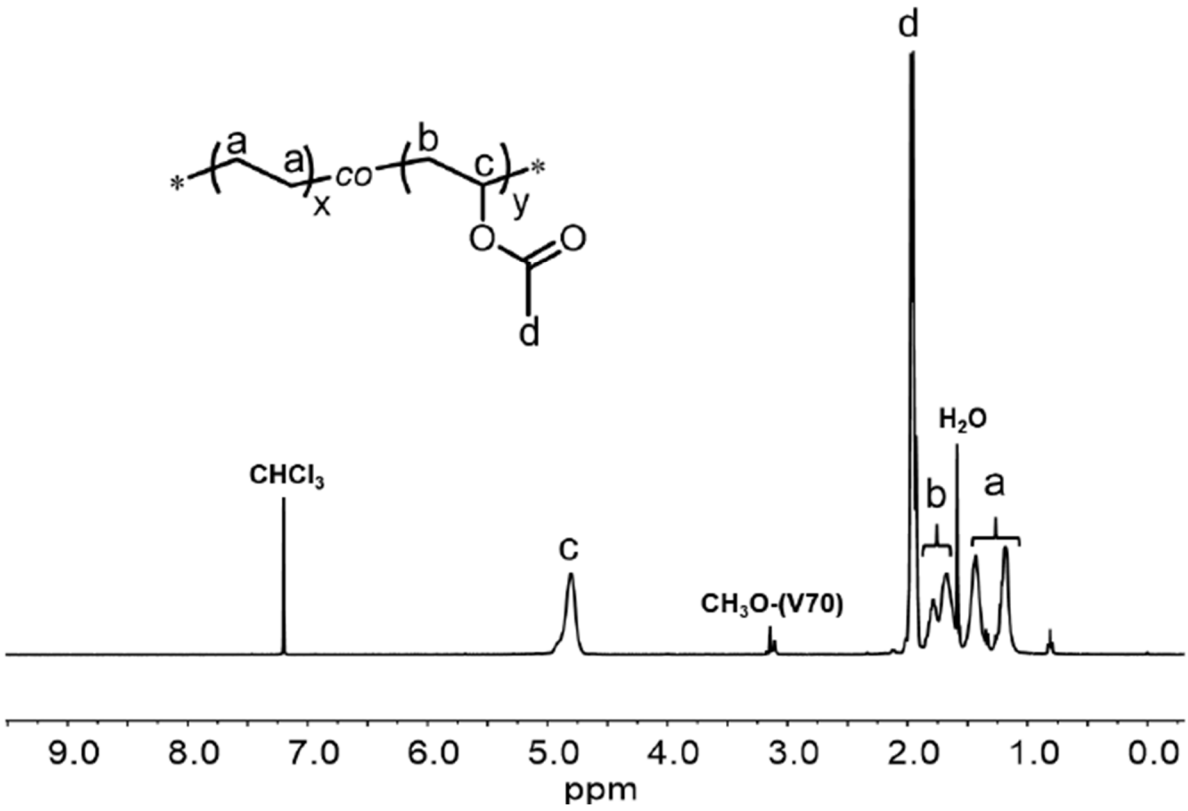

Figure S1. ^{1}H NMR spectrum of P($E_{0.31}$-*co*-$VAc_{0.69}$) (**Table 1** entry 1, M_n = 25500 g/mol, F_E = 0.31) in $CDCl_3$.

Published in : Macromolecules (2021), vol.54, n°22, pp. 10415–10427
DOI: 10.1021/acs.macromol.1c01895
Status : Postprint (Author's version)

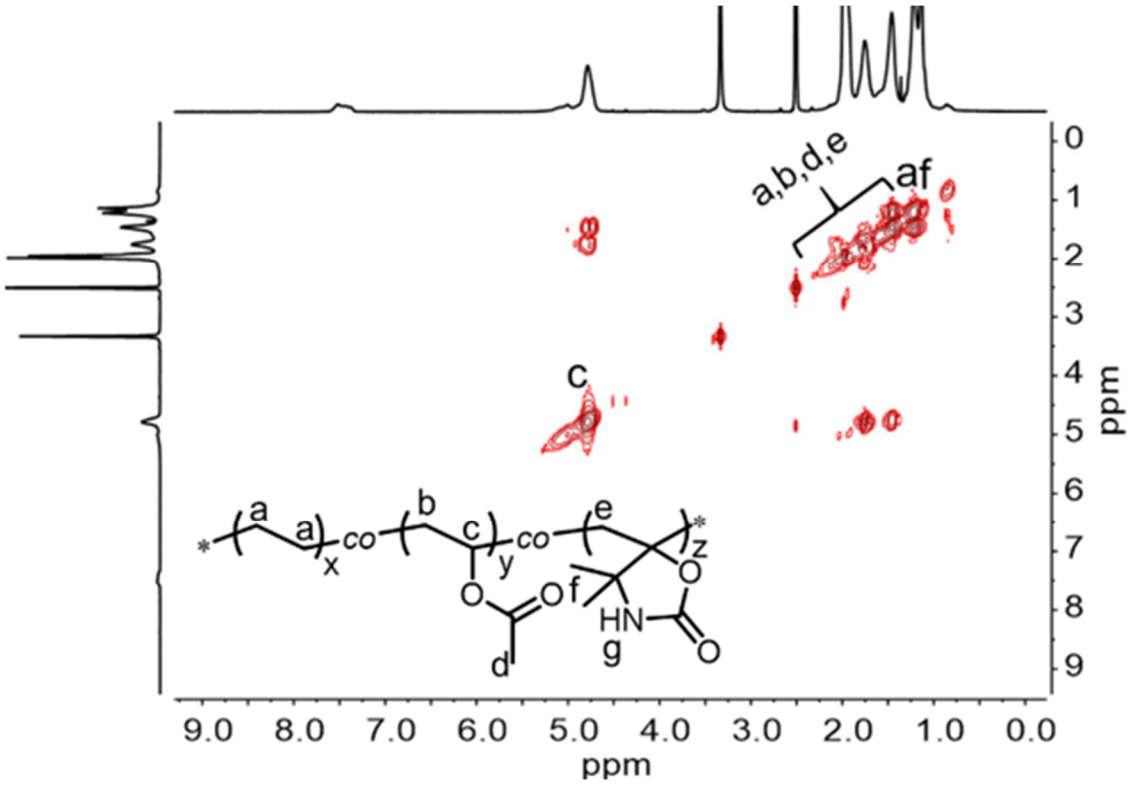

Figure S2. COSY spectrum in DMSO-d_6 of P($E_{0.34}$-*co*-$VAc_{0.55}$-*co*-$DMOx_{0.11}$) prepared by conventional radical polymerization (**Table 1**, entry 4).

Published in : Macromolecules (2021), vol.54, n°22, pp. 10415–10427
DOI: 10.1021/acs.macromol.1c01895
Status : Postprint (Author's version)

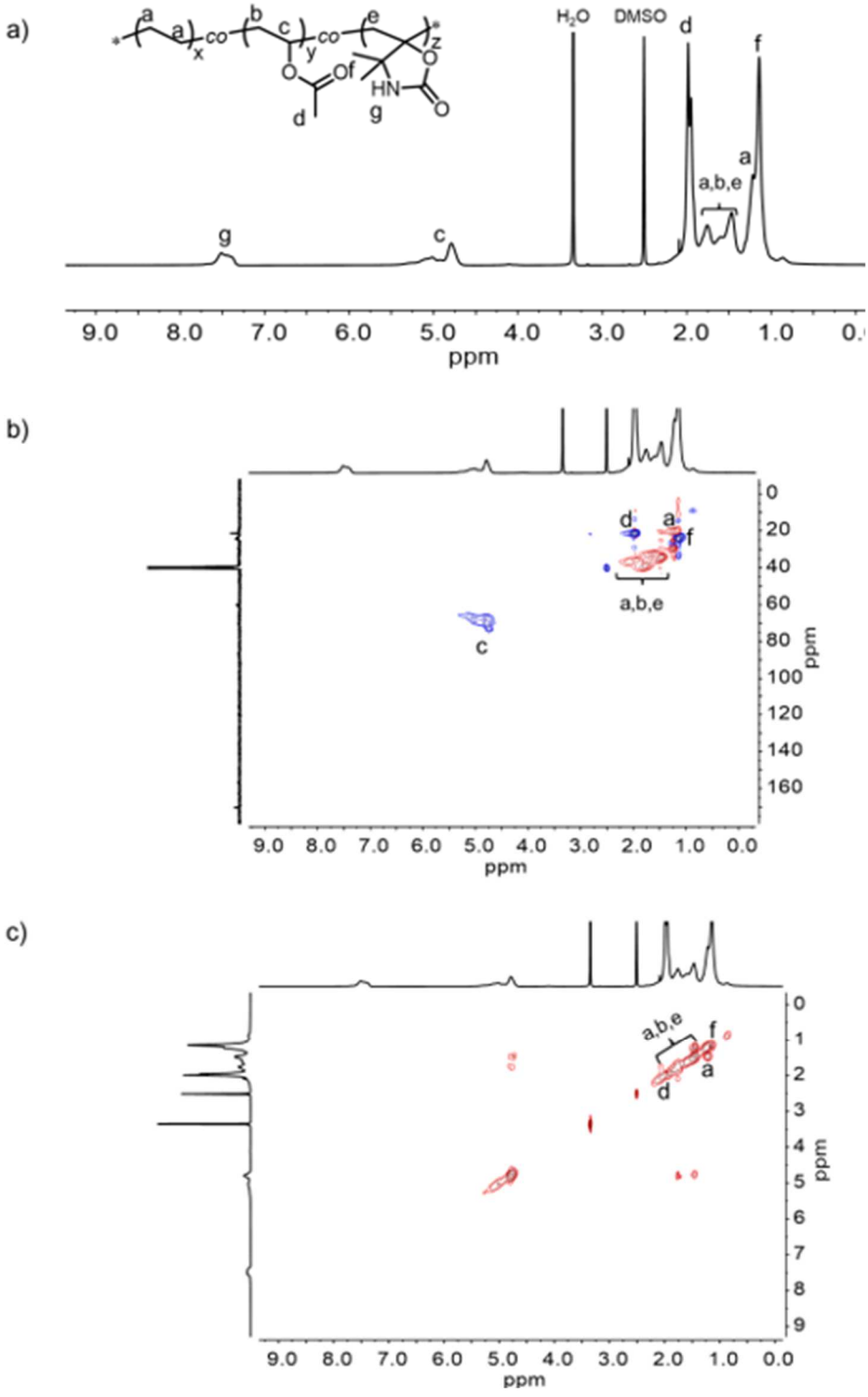

Figure S3. ^{1}H NMR (a) and HSQC (b) COSY (c) spectra in DMSO-d_6 of P($E_{0.30}$-*co*-$VAc_{0.46}$*co*-$DMOx_{0.24}$) (**Table 1**, entry 5).

Published in : Macromolecules (2021), vol.54, n°22, pp. 10415–10427
DOI: 10.1021/acs.macromol.1c01895
Status : Postprint (Author's version)

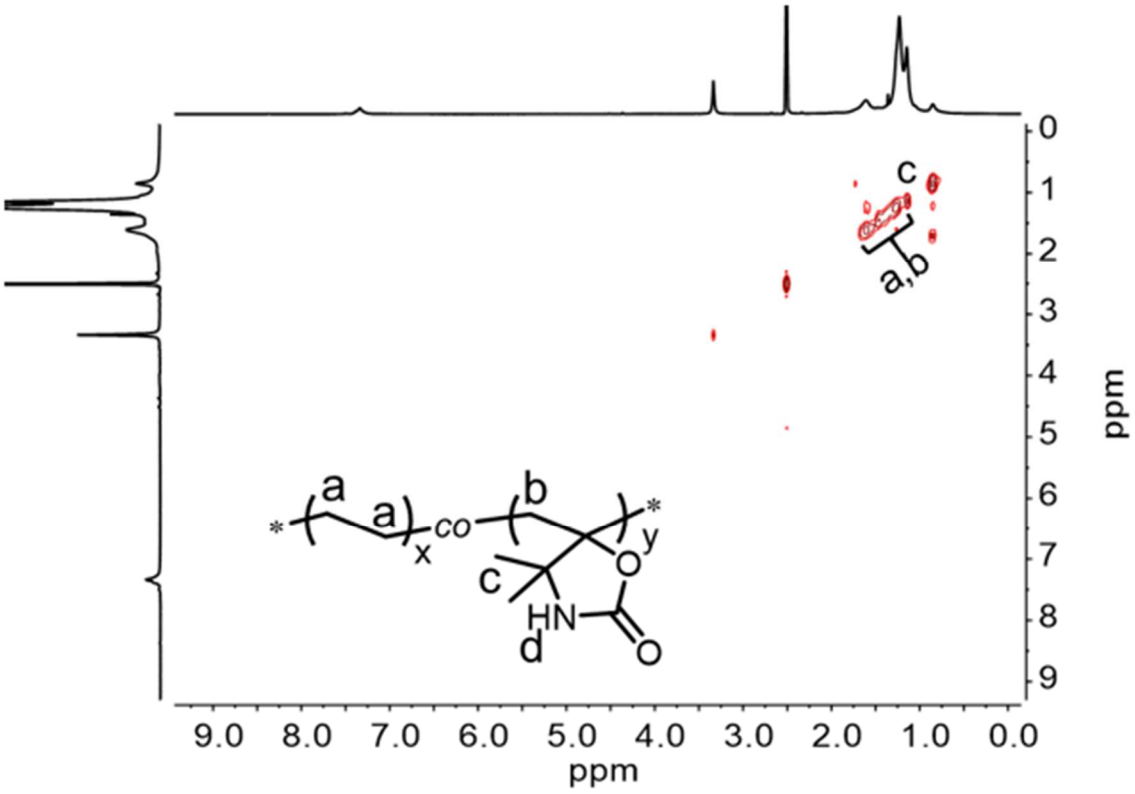

Figure S4. COSY spectrum in DMSO-d_6 of P($E_{0.74}$-*co*-$DMOx_{0.26}$) (Mn = 5100 g/mol, F_{DMOx} = 0.26) prepared by conventional radical polymerization (**Table 1**, entry 7).

Published in : Macromolecules (2021), vol.54, n°22, pp. 10415–10427
DOI: 10.1021/acs.macromol.1c01895
Status : Postprint (Author's version)

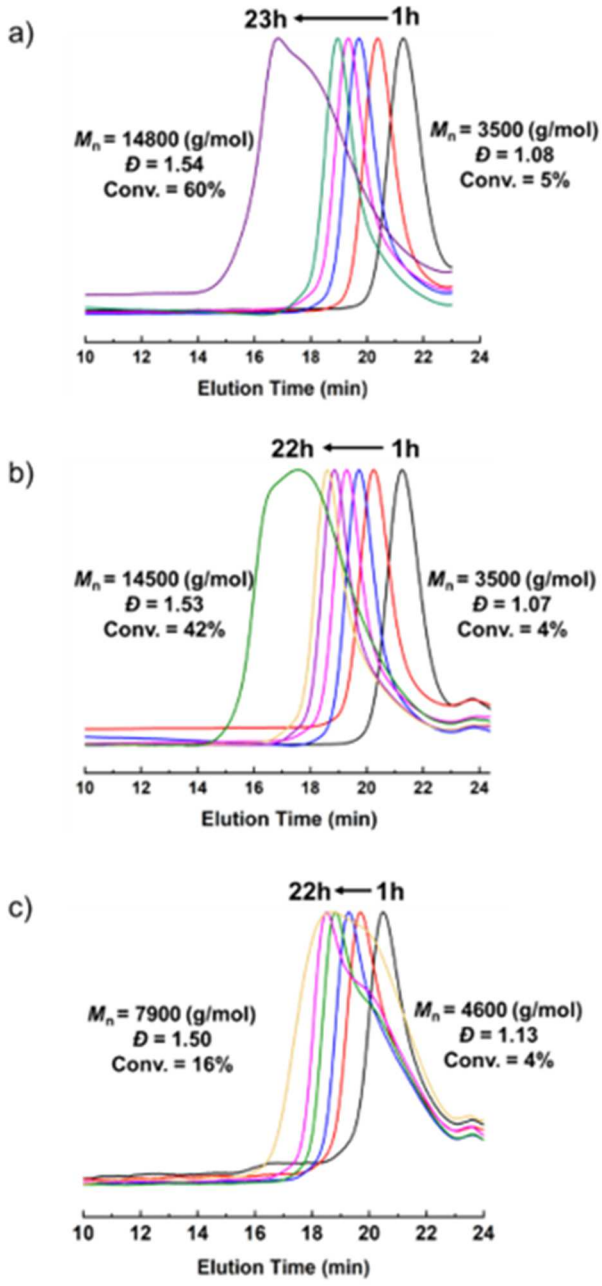

Figure S5. SEC traces for the OMRP of E/VAc/DMOx with different compositions (a and b, $f°_{DMOx}$ = 0.2 and 0.4, respectively, **Table 2** entries 1 and 2) and for the OMRP of E/DMOx (c) (**Table 2**, entry 3).

Published in : Macromolecules (2021), vol.54, n°22, pp. 10415–10427
DOI: 10.1021/acs.macromol.1c01895
Status : Postprint (Author's version)

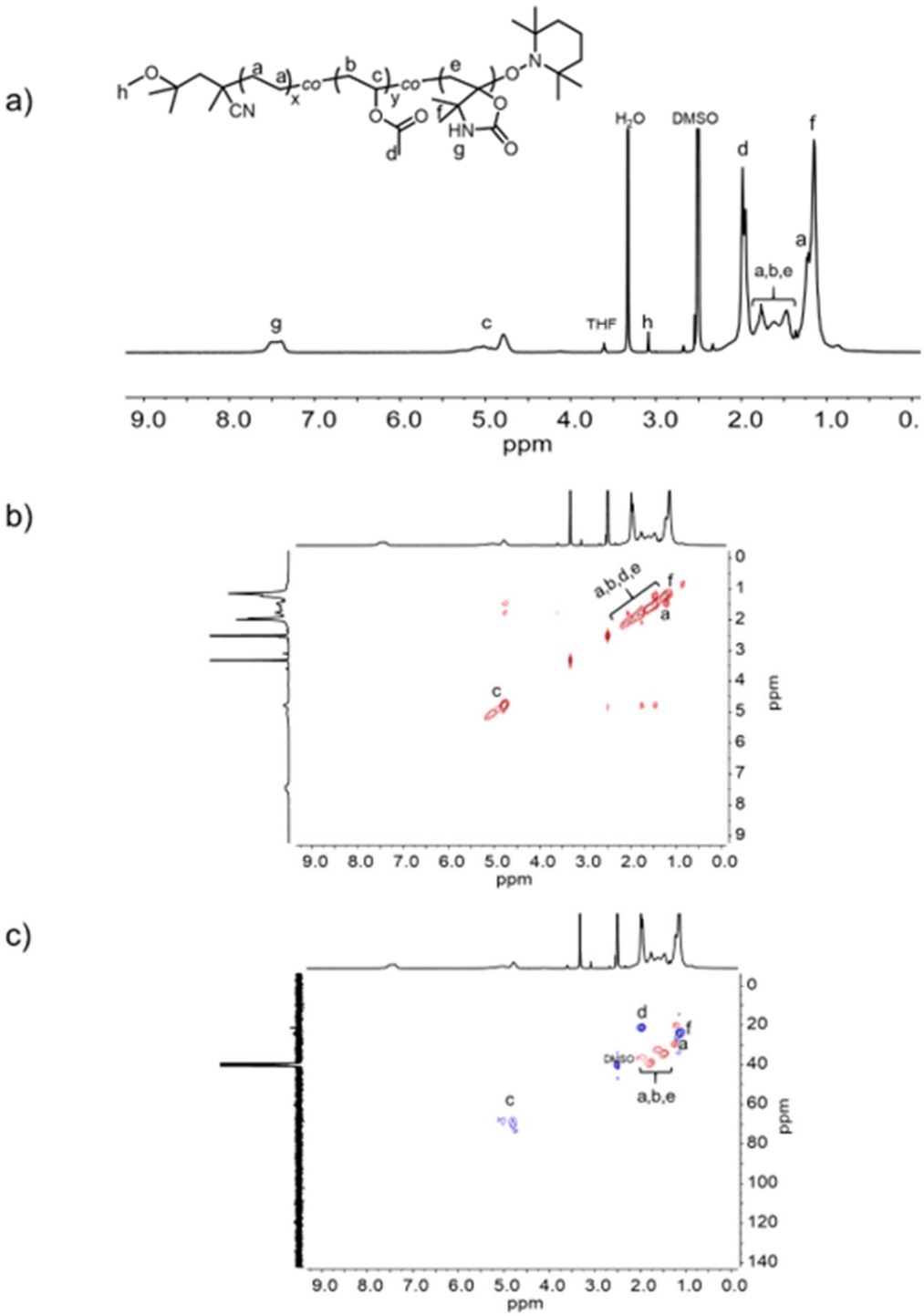

Figure S6. ^{1}H NMR (a), COSY (b) and HSQC (c) spectra in DMSO-d_6 of P(E-*co*-VAc-*co*DMOx) (M_n = 14500 g/mol, F_{DMOx} = 0.25) prepared by OMRP (**Table 2**, entry 2). The final copolymer was treated with TEMPO at the end of the OMRP in order to quench the reaction and replace the terminal cobalt complex according a well-established procedure (see *Macromolecules* **2005**, *38*, 5452-5458).

Published in : Macromolecules (2021), vol.54, n°22, pp. 10415–10427
DOI: 10.1021/acs.macromol.1c01895
Status : Postprint (Author's version)

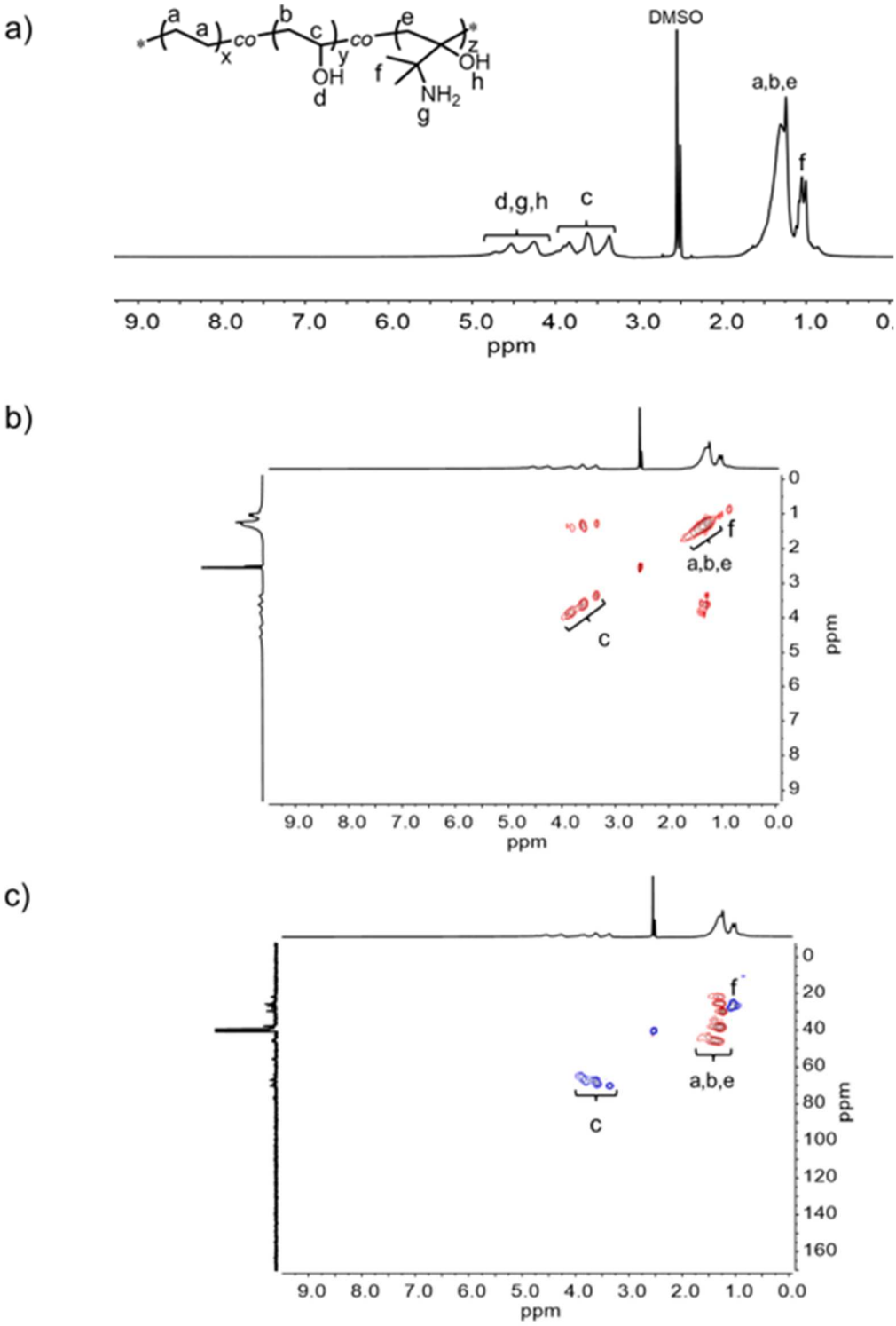

Figure S7. ^{1}H NMR (a), COSY (b) and HSQC (c) spectra in DMSO-d_6 of P($E_{0.34}$-*co*-$VOH_{0.55}$*co*-$AMBO_{0.11}$) obtained by hydrolysis of P($E_{0.34}$-*co*-$VAc_{0.55}$-*co*-$DMOx_{0.11}$) (**Table 1**, entry 4).

Published in : Macromolecules (2021), vol.54, n°22, pp. 10415–10427
DOI: 10.1021/acs.macromol.1c01895
Status : Postprint (Author's version)

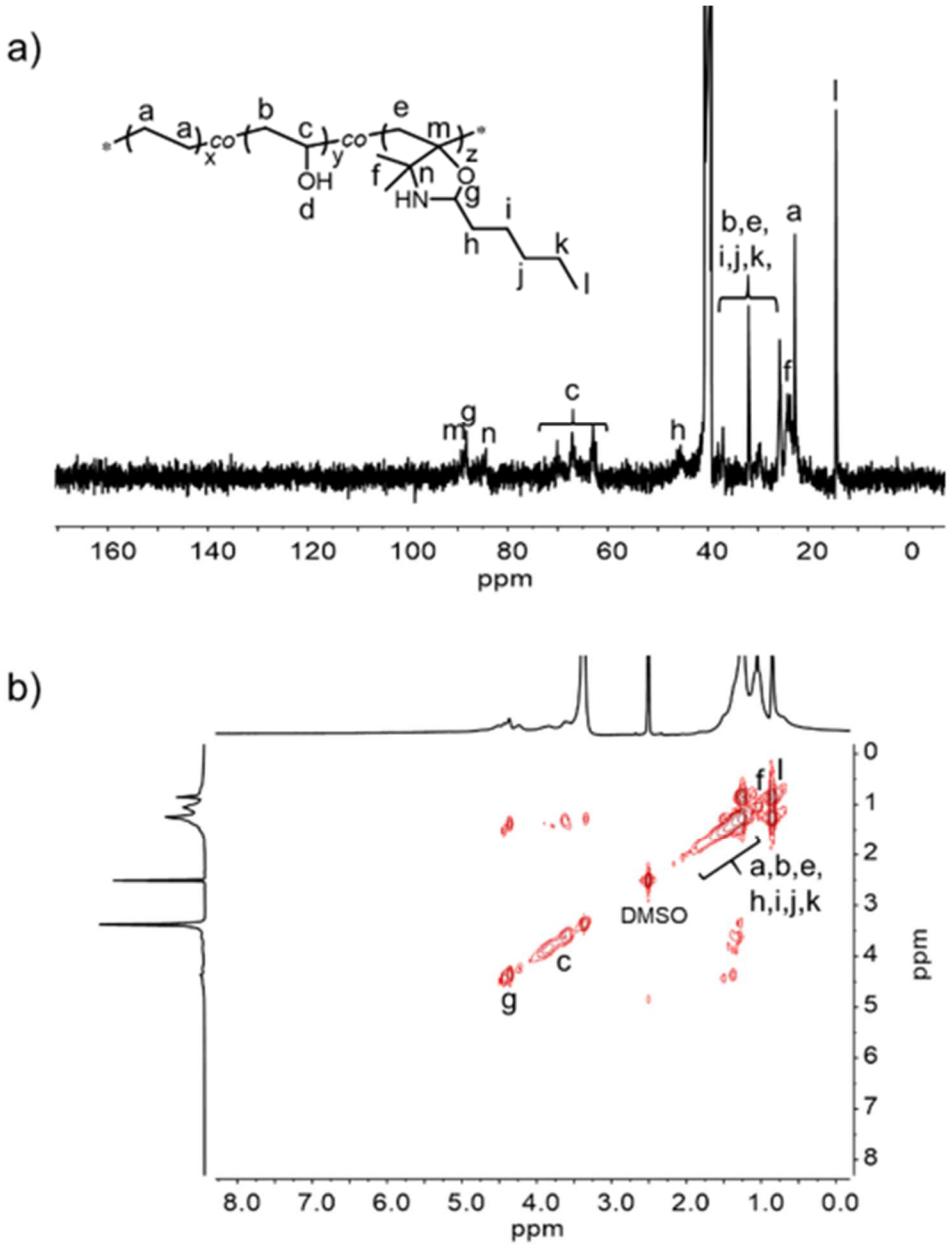

Figure S8. $^{13}C\{^{1}H\}$ NMR (a) and COSY (b) spectra of P($E_{0.30}$-*co*-$VOH_{0.46}$-*co*-$POx_{0.24}$) in DMSO-d_6.

Published in : Macromolecules (2021), vol.54, n°22, pp. 10415–10427
DOI: 10.1021/acs.macromol.1c01895
Status : Postprint (Author's version)

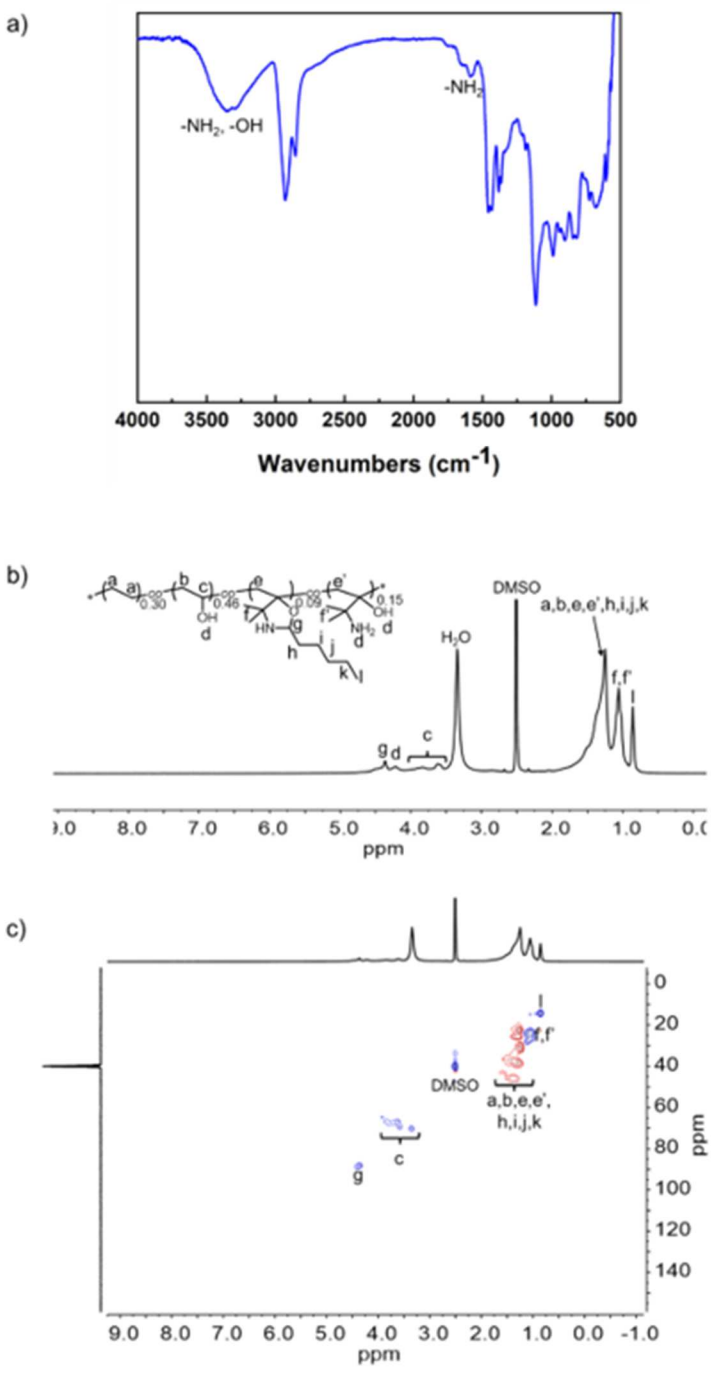

Figure S9. FTIR spectra (a), ^{1}H NMR (b) and HSQC (c) of P($E_{0.30}$-*co*-$VOH_{0.46}$-*co*-$POx_{0.24}$) after acid treatment and partial hydrolysis of the oxazolidines functions.

Published in : Macromolecules (2021), vol.54, n°22, pp. 10415–10427
DOI: 10.1021/acs.macromol.1c01895
Status : Postprint (Author's version)

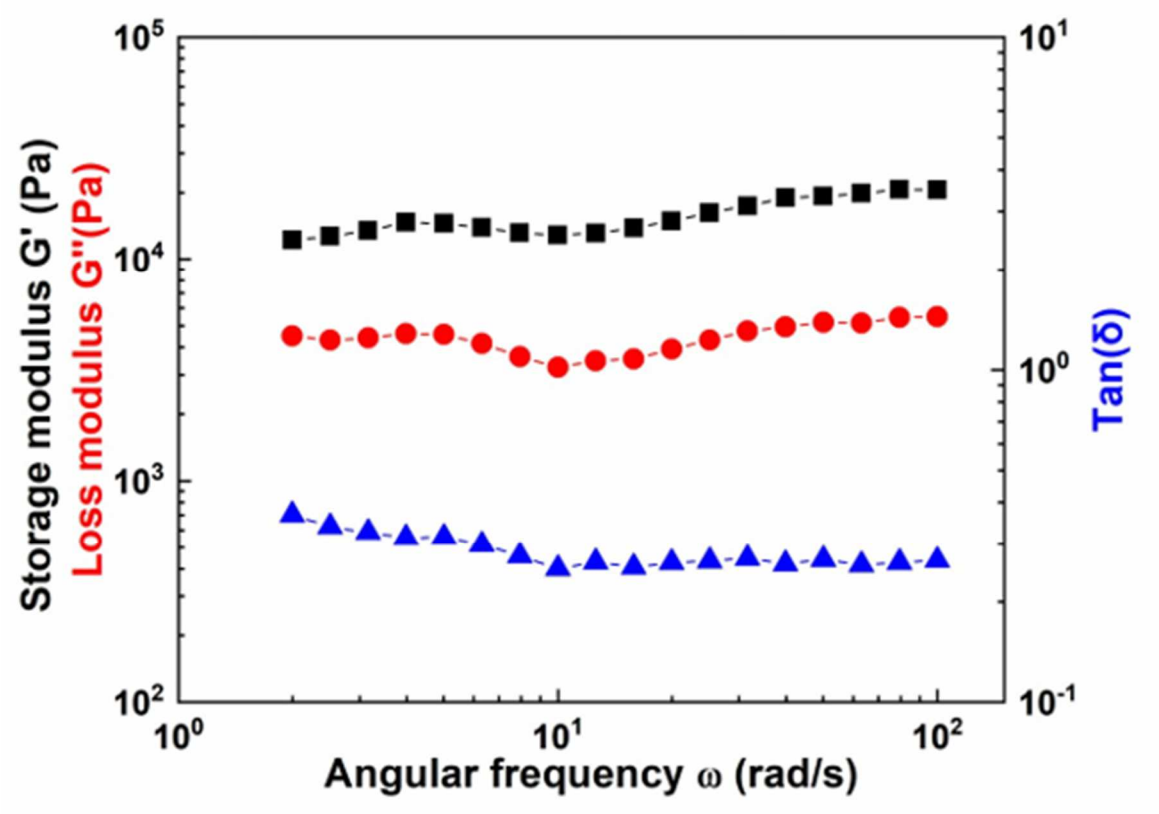

Figure S10. Frequency sweep experiment carried out on the EVOH gel resulting from the crosslinking of P($E_{0.30}$-*co*-$VOH_{0.46}$-*co*-$AMBO_{0.24}$) with glutaraldehyde in ethanol. G', G'' and tan(δ) are plotted as a function of ω.

Published in : Macromolecules (2021), vol.54, n°22, pp. 10415–10427
DOI: 10.1021/acs.macromol.1c01895
Status : Postprint (Author's version)

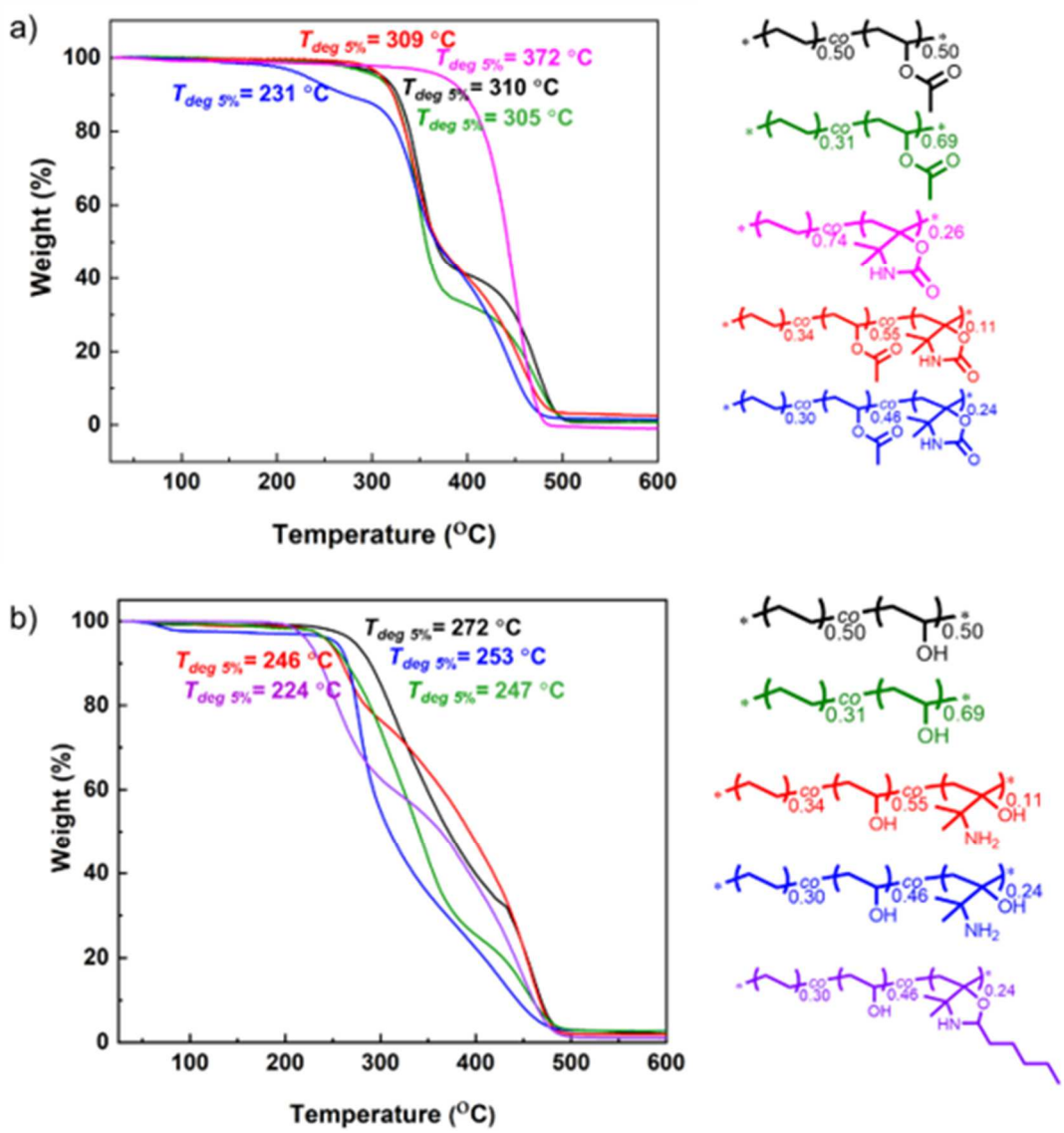

Figure S11. Thermogravimetric analysis (TGA) curves of the EVA (a) and EVOH (b) derivatives.

Published in : Macromolecules (2021), vol.54, n°22, pp. 10415–10427
DOI: 10.1021/acs.macromol.1c01895
Status : Postprint (Author's version)

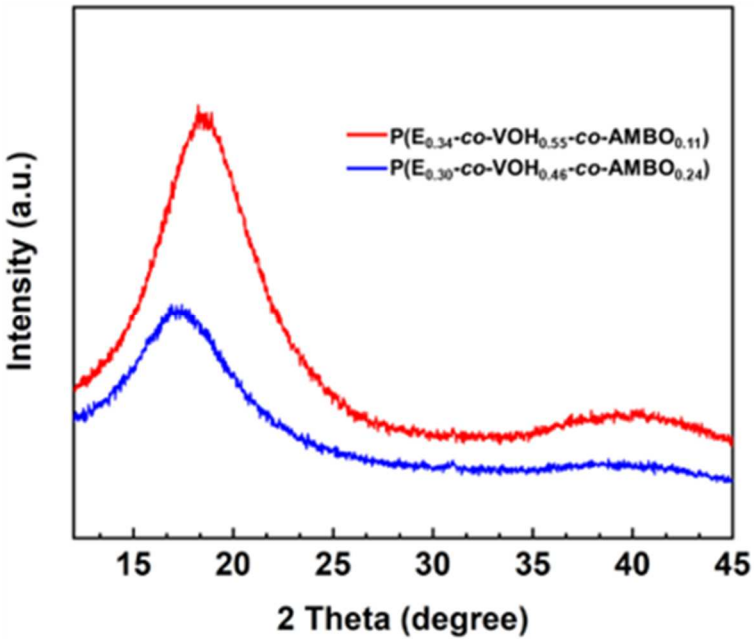

Figure S12. X-ray diffractograms of the P(E-*co*-VOH-*co*-AMBO) samples. The full width at half maximum of ~5°2θ indicates the absence of long range order characteristic of amorphous materials.

Author Information

CORRESPONDING AUTHOR

Antoine Debuigne − Center for Education and Research on Macromolecules (CERM), CESAM Research Unit, Department of Chemistry, University of Liege, 4000 Liège, Belgium

AUTHORS

Zhuoqun Wang − Center for Education and Research on Macromolecules (CERM), CESAM Research Unit, Department of Chemistry, University of Liege, 4000 Liège Belgium;
Bénédicte Vertruyen – LCIS-GreenMAT, CESAM Research Unit, Department of Chemistry, University of Liege, 4000 Liège, Belgium
Hamid Taghipour − Center for Education and Research on Macromolecules (CERM), CESAM Research Unit, Department of Chemistry, University of Liege, 4000 Liège, Belgium;
Christophe Detrembleur − Center for Education and Research on Macromolecules (CERM), CESAM Research Unit, Department of Chemistry, University of Liege, 4000 Liège, Belgium;

NOTES

The authors declare no competing financial interest.

Published in : Macromolecules (2021), vol.54, n°22, pp. 10415–10427
DOI: 10.1021/acs.macromol.1c01895
Status : Postprint (Author's version)

Acknowledgments

The authors thank the "Fonds National pour la Recherche Scientifique" (F.R.S.-FNRS) and the Fonds Wetenschappelijk Onderzoek-Vlaanderen (FWO) for financial support in the frame of the EOS project no. O019618F (ID EOS: 30902231). A.D. and C.D. are FNRS Senior Research Associate and Research Director, respectively, and thank FNRS for financial support. The authors also thank Prof. Alejandro J Müller (University of the Basque Country UPV/EHU, Donostia-San Sebastián, Spain), Prof Gwilherm Evano (Université libre de Bruxelles, Belgium), and Dr. J.-M. Thomassin for fruitful discussion.

References

(1) Mokwena, K. K.; Tang, J. Ethylene Vinyl Alcohol: A Review of Barrier Properties for Packaging Shelf Stable Foods. *Crit. Rev. Food Sci. Nutr.* 2012, 52, 640−650.

(2) Maes, C.; Luyten, W.; Herremans, G.; Peeters, R.; Carleer, R.; Buntinx, M. Recent Updates on the Barrier Properties of Ethylene Vinyl Alcohol Copolymer (EVOH): A Review. *Polym. Rev.* 2018, 58, 209−246.

(3) López-Rubio, A.; Lagaron, J. M.; Cava, D.; Hernandez-Muñoz, P.; Yamamoto, T.; Gavara, R. Morphological Alterations Induced by Temperature and Humidity in Ethylene−Vinyl Alcohol Copolymers. *Macromolecules* 2003, 36, 9467−9476.

(4) Artzi, N.; Narkis, M.; Siegmann, A. Review of Melt-Processed Nanocomposites Based on EVOH/Organoclay. *J. Polym. Sci., Part B: Polym. Phys.* 2005, 43, 1931−1943.

(5) Lagarón, J. M.; Giménez, E.; Saura, J. J.; Gavara, R. Phase Morphology, Crystallinity and Mechanical Properties of Binary Blends of High Barrier Ethylene-Vinyl Alcohol Copolymer and Amorphous Polyamide and a Polyamide-Containing Ionomer. *Polymer* 2001, 42, 7381−7394.

(6) Marconi, W.; Cordelli, S.; Napoli, A.; Piozzi, A. Polymeric Systems Based on Derivatives of Ethylene-Vinyl Alcohol Copolymers. *J. Bioact. Compat. Polym.* 2000, 15, 257−271.

(7) Young, T.-H.; Yao, C.-H.; Sun, J.-S.; Lai, C.-P.; Chen, L.-W. The Effect of Morphology Variety of EVAL Membranes on the Behavior of Myoblasts in Vitro. *Biomaterials* 1998, 19, 717−724.

(8) Avramescu, M. E.; Sager, W. F. C.; Wessling, M. Functionalised Ethylene Vinyl Alcohol Copolymer (EVAL) Membranes for Affinity Protein Separation. *J. Membr. Sci.* 2003, 216, 177−193.

(9) Young, T.-H.; Lin, C.-W.; Cheng, L.-P.; Hsieh, C.-C. Preparation of EVAL Membranes with Smooth and Particulate Morphologies for Neuronal Culture. *Biomaterials* 2001, 22, 1771−1777.

(10) Young, T.; Chuang, W. Y.; Wei, C. W.; Tang, C. Y. Investigation of the Drug Distribution and Release Characteristics from Particulate Membranes. *J. Membr. Sci.* 2001, 191, 199−205.

(11) Sheng, S.; YIn, X.; Chen, F.; Lv, Y.; Zhang, L.; Cao, M.; Sun, Y. Preparation and Characterization of PVA-Co-PE Drug-Loaded Nanofiber Membrane by Electrospinning Technology. *AAPS PharmSciTech* 2020, 21, 199−208.

(12) Fu, Q.; Si, Y.; Liu, L.; Yu, J.; Ding, B. Elaborate Design of Ethylene Vinyl Alcohol (EVAL) Nanofiber-Based Chromatographic Media for Highly Efficient Adsorption and Extraction of Proteins. *J. Colloid Interface Sci.* 2019, 555, 11−21.

(13) Zhu, J.; Yang, J.; Sun, G. Cibacron Blue F3GA functionalized poly(vinyl alcohol-co-ethylene) (PVA-co-PE) nanofibrous membranes as high efficient affinity adsorption materials. *J. Membr. Sci.* 2011, 385−386, 269−276.

(14) Avramescu, M.-E.; Girones, M.; Borneman, Z.; Wessling, M. Preparation of Mixed Matrix Adsorber Membranes for Protein Recovery. *J. Membr. Sci.* 2003, 218, 219−233.

(15) Lu, Y.; Wu, Z.; Li, M.; Liu, Q.; Wang, D. Hydrophilic PVA-coPE Nanofiber Membrane Functionalized with Iminodiacetic Acid by Solid-Phase Synthesis for Heavy Metal Ions Removal. *React. Funct. Polym.* 2014, 82, 98−102.

(16) Muriel-Galet, V.; Talbert, J. N.; Gavara, R.; Goddard, J. M. Covalent Immobilization of Lysozyme on Ethylene Vinyl Alcohol Films for Nonmigrating Antimicrobial Packaging Applications. *J. Agric. Food Chem.* 2013, 61, 6720−6727.

(17) Bellusci, M.; Francolini, I.; Martinelli, A.; D'Ilario, L.; Piozzi, A. Lipase Immobilization on Differently Functionalized Vinyl-Based Amphiphilic Polymers: Influence of Phase Segregation on the Enzyme Hydrolytic Activity. *Biomacromolecules* 2012, 13, 805−813.

(18) Moraes, M. A. R.; Moreira, A. C. F.; Barbosa, R. V.; Soares, B. G. Graft Copolymer from Modified Ethylene−Vinyl Acetate (EVA) Copolymers. 3. Poly(EVA-g-Methyl Methacrylate) from MercaptoModified EVA. *Macromolecules* 1996, 29, 416−422.

Published in : Macromolecules (2021), vol.54, n°22, pp. 10415–10427
DOI: 10.1021/acs.macromol.1c01895
Status : Postprint (Author's version)

(19) Si, Y.; Zhang, Z.; Wu, W.; Fu, Q.; Huang, K.; Nitin, N.; Ding, B.; Sun, G. Daylight-Driven Rechargeable Antibacterial and Antiviral Nanofibrous Membranes for Bioprotective Applications. *Sci. Adv.* 2018, 4, No. eaar5931.

(20) Marconi, W.; Piozzi, A.; Marcone, R. Synthesis and Characterization of Novel Carboxylated Ethylene-Vinyl Alcohol Polymers. *Eur. Polym. J.* 2001, 37, 1021−1025.

(21) Bruzaud, S.; Levesque, G. Synthesis and Characterization of New Functional Polymers by Polymer-Analog Reactions on EVOH Copolymer. *Macromol. Chem. Phys.* 2000, 201, 1758−1764.

(22) Huang, K.; Yang, X.; Ma, Y.; Sun, G.; Nitin, N. Incorporation of Antimicrobial Bio-Based Carriers onto Poly(vinyl alcohol-co-ethylene) Surface for Enhanced Antimicrobial Activity. *ACS Appl. Mater. Interfaces* 2021, 13, 36275−36285.

(23) Wang, W.; Zhang, H.; Zhang, Z.; Luo, M.; Wang, Y.; Liu, Q.; Chen, Y.; Li, M.; Wang, D. Amine-Functionalized PVA-Co-PE Nanofibrous Membrane as Affinity Membrane with High Adsorption Capacity for Bilirubin. *Colloids Surf.*, B 2017, 150, 271−278.

(24) Jiang, H.; Wu, P.; Yang, Y. Variable Temperature FTIR Study of Poly(Ethylene-co-Vinyl Alcohol)-Graft-Poly(ε-Caprolactone). *Biomacromolecules* 2003, 4, 1343−1347.

(25) Wang, X. L.; Du, F. G.; Meng, Y. Z.; Li, R. K. Y. Novel in Situ Crosslinking Reaction of Ethylene-Vinyl Alcohol Copolymers by Propylene Carbonate. *Mater. Lett.* 2006, 60, 509−513.

(26) Sánchez-Chaves, M.; Ruiz, C.; Cerrada, M. L.; FernándezGarcía, M. Novel Glycopolymers Containing Aminosaccharide Pendant Groups by Chemical Modification of Ethylene − Vinyl Alcohol Copolymers. *Polymer* 2008, 49, 2801−2807.

(27) Cerrada, M. L.; Ruiz, C.; Sánchez-Chaves, M.; FernándezGarcía, M. Molecular Recognition Capability and Rheological Behavior in Solution of Novel Lactone-Based Glycopolymers. *Eur. Polym. J.* 2009, 45, 3176−3186.

(28) Nechikkattu, R.; Athiyanathil, S. Thermo-Responsive Poly(Ethylene-co-Vinyl Alcohol) Based Asymmetric Membranes. *RSC Adv.* 2016, 6, 114276−114285.

(29) Luft, G.; Stein, F.; Dorn, M. The Free-Radical Terpolymerization of Ethylene, Methyl Acrylate, and Vinyl Acetate at High Pressure. Angew. Makromol. *Chem.* 1993, 211, 131−140.

(30) Luft, G.; Stein, F.; Dorn, M. Radical Terpolymerization of Ethylene, Methyl Acrylate and Vinyl Acetate under High Pressure Physical Properties of the Polymers. Angew. Makromol. *Chem.* 1993, 207, 145−155.

(31) Buback, M.; Panten, K. Terpolymerization of Ethene, Acrylonitrile and Vinyl Acetate. *Makromol. Chem.* 1993, 194, 2471− 2481.

(32) Akkapeddi, M. K. Poly(α-Methylene-γ-Butyrolactone) Synthesis, Configurational Structure, and Properties. *Macromolecules* 1979, 12, 546−551.

(33) Vobecka, Z.; Wei, C.; Tauer, K.; Esposito, D. Poly(αmethylene-γ-valerolactone) 1. Sustainable monomer synthesis and radical polymerization studies. *Polymer* 2015, 74, 262−271.

(34) Ding, K.; John, A.; Shin, J.; Lee, Y.; Quinn, T.; Tolman, W. B.; Hillmyer, M. A. High-Performance Pressure-Sensitive Adhesives from Renewable Triblock Copolymers. *Biomacromolecules* 2015, 16, 2537− 2539.

(35) Trotta, J. T.; Jin, M.; Stawiasz, K. J.; Michaudel, Q.; Chen, W.L.; Fors, B. P. Synthesis of Methylene Butyrolactone Polymers from Itaconic Acid. *J. Polym. Sci., Part A: Polym. Chem.* 2017, 55, 2730− 2737.

(36) Xu, S.; Huang, J.; Xu, S.; Luo, Y. RAFT Ab Initio Emulsion Copolymerization of γ-Methyl-α- Methylene-γ-Butyrolactone and Styrene. *Polymer* 2013, 54, 1779−1785.

(37) Pittman, C. U.; Lee, H. Radical-Initiated Polymerization of βMethyl-α-Methylene-γ-Butyrolactone. *J. Polym. Sci., Part A: Polym. Chem.* 2003, 41, 1759−1777.

(38) Kollár, J.; Mrlík, M.; Moravcíková, D.; Kroneková, Z.; Liptaǰ, T.; Lacík, I.; Mosnácek, J̌ . Tulips: A Renewable Source of Monomer for Superabsorbent Hydrogels. Macromolecules 2016, 49, 4047−4056. (39) Ramram, M. B.; Chen, D.; Ma, Y.; Wang, L.; Yang, W. Stabilizer-free precipitation copolymerization of renewable bio-based α-methylene-γ-butyrolactone and styrene. *J. Macromol. Sci., Part A: Pure Appl.Chem.* 2016, 53, 484−491.

(40) Cockburn, R. A.; Siegmann, R.; Payne, K. A.; Beuermann, S.; McKenna, T. F. L.; Hutchinson, R. A. Free Radical Copolymerization Kinetics of γ-Methyl-α-methylene-γ-butyrolactone (MeMBL). *Biomacromolecules* 2011, 12, 2319−2326.

(41) Miyake, G. M.; Zhang, Y.; Chen, E. Y.-X. Polymerizability of Exo -methylene-lactide toward vinyl addition and ring opening. *J. Polym. Sci., Part A: Polym. Chem.* 2015, 53, 1523−1532.

(42) Heyns, I. M.; Pfukwa, R.; Klumperman, B. Synthesis, Characterization, and Evaluation of Cytotoxicity of Poly(3-Methylene-2-Pyrrolidone). *Biomacromolecules* 2016, 17, 1795−1800.

(43) Mosnáček, J.; Matyjaszewski, K. Atom Transfer Radical Polymerization of Tulipalin A: A Naturally Renewable Monomer. *Macromolecules* 2008, 41, 5509−5511.

(44) Mosnáček, J.; Yoon, J. A.; Juhari, A.; Koynov, K.; Matyjaszewski, K. Synthesis, morphology and mechanical properties of linear triblock copolymers based on poly(α-methylene-γ-butyrolactone). *Polymer* 2009, 50, 2087−2094.

(45) Scholten, P. B. V.; Grignard, B.; Debuigne, A.; Cramail, H.; Meier, M. A. R.; Detrembleur, C. Functional Polyethylenes by Organometallic-Mediated Radical Polymerization of Biobased Carbonates. *ACS Macro Lett.* 2021, 10, 313−320.

Published in : Macromolecules (2021), vol.54, n°22, pp. 10415–10427
DOI: 10.1021/acs.macromol.1c01895
Status : Postprint (Author's version)

(46) Scholten, P. B. V.; Gennen, S.; De Winter, J.; Grignard, B.; Debuigne, A.; Meier, M. A. R.; Detrembleur, C. Merging CO_2-Based Building Blocks with Cobalt-Mediated Radical Polymerization for the Synthesis of Functional Poly(Vinyl Alcohol)S. *Macromolecules* 2018, 51, 3379−3393.

(47) Wang, Z.; Poli, R.; Detrembleur, C.; Debuigne, A. Organometallic-Mediated Radical (Co)polymerization of γ-Methylene-γ-Butyrolactone: Access to pH-Responsive Poly(vinyl alcohol) Derivatives. *Macromolecules* 2019, 52, 8976−8988.

(48) Wang, Z.; Detrembleur, C.; Debuigne, A. Reversible Deactivation Radical (Co)Polymerization of Dimethyl Methylene Oxazolidinone towards Responsive Vicinal Aminoalcohol-Containing Copolymers. *Polym. Chem.* 2020, 11, 7207−7220.

(49) Mullen, B.; Rodwogin, M.; Stollmaier, F.; Yontz, D.; Leibig, C. New Bio-Derived Superabsorbents from Nature. *Green Mater. 2013*, 1, 186−190.

(50) Debuigne, A.; Champouret, Y.; Jérôme, R.; Poli, R.; Detrembleur, C. Mechanistic Insights into the Cobalt-Mediated Radical Polymerization (CMRP) of Vinyl Acetate with Cobalt(III) Adducts as Initiators. *Chem.-Eur. J.* 2008, 14, 4046−4059.

(51) Ishida, T.; Kikuchi, S.; Tsubo, T.; Yamada, T. Silver-Catalyzed Incorporation of Carbon Dioxide into o-Alkynylaniline Derivatives. Org. Lett. 2013, 15, 848−851.

(52) Yoshida, M.; Mizuguchi, T.; Shishido, K. Synthesis of Oxazolidinones by Efficient Fixation of Atmospheric CO_2 with Propargylic Amines by Using a Silver/1,8-Diazabicyclo[5.4.0] Undec7-Ene (DBU) Dual-Catalyst System. *Chem.-Eur. J.* 2012, 18, 15578−15581.

(53) Grau, E.; Broyer, J.-P.; Boisson, C.; Spitz, R.; Monteil, V. Unusual Activation by Solvent of the Ethylene Free Radical Polymerization. *Polym. Chem.* 2011, 2, 2328−2333.

(54) Demarteau, J.; Debuigne, A.; Detrembleur, C. Organocobalt Complexes as Sources of Carbon-Centered Radicals for Organic and Polymer Chemistries. *Chem. Rev.* 2019, 119, 6906−6955.

(55) Debuigne, A.; Jérôme, C.; Detrembleur, C. OrganometallicMediated Radical Polymerization of "Less Activated Monomers": Fundamentals, Challenges and Opportunities. *Polymer* 2017, 115, 285−307.

(56) Allan, L. E. N.; Perry, M. R.; Shaver, M. P. Organometallic Mediated Radical Polymerization. *Prog. Polym. Sci.* 2012, 37, 127− 156.

(57) Hurtgen, M.; Detrembleur, C.; Jerome, C.; Debuigne, A. Insight into Organometallic-Mediated Radical Polymerization. *Polym. Rev.* 2011, 51, 188−213.

(58) Fliedel, C.; Poli, R. Homolytically Weak Metal-Carbon Bonds Make Robust Controlled Radical Polymerizations Systems for "LessActivated Monomers. *J. Organomet. Chem.* 2019, 880, 241−252.

(59) Kermagoret, A.; Debuigne, A.; Jérôme, C.; Detrembleur, C. Precision Design of Ethylene- and Polar-Monomer-Based Copolymers by Organometallic-Mediated Radical Polymerization. *Nat. Chem.* 2014, 6, 179−187.

(60) Demarteau, J.; Kermagoret, A.; Jérôme, C.; Detrembleur, C.; Debuigne, A. Controlled Synthesis of Ethylene-Vinyl Acetate Based Copolymers by Organometallic Mediated Radical Polymerization. *ACS Symp. Ser.* 2015, 1188, 47−61.

(61) Demarteau, J.; De Winter, J.; Detrembleur, C.; Debuigne, A. Ethylene/Vinyl Acetate-Based Macrocycles via OrganometallicMediated Radical Polymerization and CuAAC "click" Reaction. *Polym. Chem.* 2018, 9, 273−278.

(62) Katz, S. J.; Bergmeier, S. C. Convenient Methods for the Hydrolysis of Oxazolidinones to Vicinal Aminoalcohols. *Tetrahedron Lett.* 2002, 43, 557−559.

(63) Bergmeier, S. C.; Stanchina, D. M. Synthesis of Vicinal Amino Alcohols via a Tandem Acylnitrene Aziridination-Aziridine Ring Opening. *J. Org. Chem.* 1997, 62, 4449−4456.

(64) Benakli, K.; Zha, C.; Kerns, R. J. Oxazolidinone Protected 2Amino-2-Deoxy-D-Glucose Derivatives as Versatile Intermediates in Stereoselective Oligosaccharide Synthesis and the Formation of αLinked Glycosides. *J. Am. Chem. Soc.* 2001, 123, 9461−9462.

(65) Noshita, M.; Shimizu, Y.; Morimoto, H.; Ohshima, T. Diethylenetriamine-Mediated Direct Cleavage of Unactivated Carbamates and Ureas. *Org. Lett.* 2016, 18, 6062−6065.

(66) Giovanni, M. C. D.; Misiti, D.; Villani, C.; Zappia, G. A Straightforward Synthesis of Proclavaminic Acid, a Biosynthetic Precursor of Clavulanic Acid. *Tetrahedron: Asymmetry* 1996, 7, 2277− 2286.

(67) Barbera, V.; Leonardi, G.; Valerio, A. M.; Rubino, L.; Sun, S.; Famulari, A.; Galimberti, M.; Citterio, A.; Sebastiano, R. Environmentally Friendly and Regioselective One-Pot Synthesis of Imines and Oxazolidines Serinol Derivatives and Their Use for Rubber Cross-Linking. *ACS Sustainable Chem. Eng.* 2020, 8, 9356−9366.

(68) Granvogl, M.; Beksan, E.; Schieberle, P. New Insights into the Formation of Aroma-Active Strecker Aldehydes from 3-Oxazolines as Transient Intermediates. *J. Agric. Food Chem.* 2012, 60, 6312−6322.

(69) Johansen, M.; Bundgaard, H. Prodrugs as Drug Delivery Systems XXV: Hydrolysis of Oxazolidines-a Potential New Prodrug Type. *J. Pharm. Sci.* 1983, 72, 1294−1298.

(70) McClelland, R. A.; Somani, R. Kinetic Analysis of the Ring Opening of an N-Alkyloxazolidine. Hydrolysis of 2-(4-Methylphenyl)2,3-Dimethyl-1,3-Oxazolidine. *J. Org. Chem.* 1981, 46, 4345−4350.

Published in : Macromolecules (2021), vol.54, n°22, pp. 10415–10427
DOI: 10.1021/acs.macromol.1c01895
Status : Postprint (Author's version)

(71) Cui, Q.; Wu, F.; Wang, E. Novel Amphiphilic Diblock Copolymers Bearing Acid-Labile Oxazolidine Moieties: Synthesis, Self-Assembly and Responsive Behavior in Aqueous Solution. *Polymer* 2011, 52, 1755−1765.
(72) Yuan, L.; Qiang, P.; Gao, J.; Shi, Y. Synthesis of Oxazolidines as Latent Curing Agents for Single-Component Polyurethane Adhesive and Its Properties Study. *J. Appl. Polym. Sci.* 2018, 135, 45722.
(73) Yamaki, S. B.; Prado, E. A.; Atvars, T. D. Z. Phase Transitions and Relaxation Processes in Ethylene-Vinyl Acetate Copolymers Probed by Fluorescence Spectroscopy. *Eur. Polym. J.* 2002, 38, 1811− 1826.
(74) Rimez, B.; Rahier, H.; Van Assche, G.; Artoos, T.; Van Mele, B. The Thermal Degradation of Poly(Vinyl Acetate) and Poly(Ethyleneco-Vinyl Acetate), Part II: Modelling the Degradation Kinetics. *Polym. Degrad. Stab.* 2008, 93, 1222−1230.
(75) Alvarez, V. A.; Ruseckaite, R. A.; Vázquez, A. Kinetic Analysis of Thermal Degradation in Poly(Ethylene− Vinyl Alcohol) Copolymers. *J. Appl. Polym.* Sci. 2003, 90, 3157−3163.